



Fundação
para a Ciência
e a Tecnologia



LABORATÓRIO DE INSTRUMENTAÇÃO
E FÍSICA EXPERIMENTAL DE PARTÍCULAS

BFKL and low- x physics

Lecture 3

(27-06-2024)

Grigorios Chachamis, LIP Lisbon

Midsummer School in QCD 2024
Saariselkä, 24 June to 6 July 2024, Finland

The BFKL equation, again

$$\begin{aligned}
 \omega F(\omega, \mathbf{k}, \mathbf{k}', \mathbf{q}) = & \delta^2(\mathbf{k} - \mathbf{k}') \\
 & + \frac{N_c \alpha_s}{2\pi^2} \int d^2\kappa \left\{ \frac{-\mathbf{q}^2}{(\kappa - \mathbf{q})^2 \mathbf{k}^2} F(\omega, \kappa, \mathbf{k}', \mathbf{q}) \right. \\
 & + \frac{1}{(\kappa - \mathbf{k})^2} \left[F(\omega, \kappa, \mathbf{k}', \mathbf{q}) - \frac{\mathbf{k}^2 F(\omega, \mathbf{k}, \mathbf{k}', \mathbf{q})}{\kappa^2 + (\mathbf{k} - \kappa)^2} \right] \\
 & + \frac{1}{(\kappa - \mathbf{k})^2} \left[\frac{(\mathbf{k} - \mathbf{q})^2 \kappa^2 F(\omega, \kappa, \mathbf{k}', \mathbf{q})}{(\kappa - \mathbf{q})^2 \mathbf{k}^2} \right. \\
 & \left. \left. - \frac{(\mathbf{k} - \mathbf{q})^2 F(\omega, \mathbf{k}, \mathbf{k}', \mathbf{q})}{(\kappa - \mathbf{q})^2 + (\mathbf{k} - \kappa)^2} \right] \right\}
 \end{aligned}$$

To complete the story...

Suppose now that we know $F(\omega, \mathbf{k}, \mathbf{k}', \mathbf{q})$

Then we take an inverse Mellin transform to go back to s-space

$$F(s, \mathbf{k}, \mathbf{k}', \mathbf{q}) = \frac{1}{2\pi i} \int_{c-i\infty}^{c+i\infty} d\omega \left(\frac{s}{|t|} \right)^\omega F(\omega, \mathbf{k}, \mathbf{k}', \mathbf{q})$$

To recover the imaginary part of the ladder diagrams all we need to do is:

$$\frac{\text{Im } \mathcal{A}_1(s, t)}{s} = (8\pi^2 \alpha_s)^2 \frac{N_c^2 - 1}{4N_c} \int \frac{d^2 \mathbf{k}}{(2\pi)^2} \int \frac{d^2 \mathbf{k}'}{(2\pi)^2} \frac{F(s, \mathbf{k}, \mathbf{k}', \mathbf{q})}{\mathbf{k}'^2 (\mathbf{k} - \mathbf{q})^2}$$

The BFKL equation for zero momentum transfer, $q=0$

$$\omega F(\omega, \mathbf{k}, \mathbf{k}') = \delta^2(\mathbf{k} - \mathbf{k}') + \frac{N_c \alpha_s}{\pi^2} \int \frac{d^2 \kappa}{(\mathbf{k} - \kappa)^2} \times \left[F(\omega, \kappa, \mathbf{k}') - \frac{\mathbf{k}^2}{\kappa^2 + (\mathbf{k} - \kappa)^2} F(\omega, \mathbf{k}, \mathbf{k}') \right]$$

Or symbolically:

$$\omega F(\omega, \mathbf{k}, \mathbf{k}') = \delta^2(\mathbf{k} - \mathbf{k}') + \int d^2 \kappa \mathcal{K}(\mathbf{k}, \kappa) F(\omega, \kappa, \mathbf{k}')$$

where $\mathcal{K}(\mathbf{k}, \kappa) = 2 \epsilon(-\mathbf{k}^2) \delta^2(\mathbf{k} - \kappa) + \frac{N_c \alpha_s}{\pi^2} \frac{1}{(\mathbf{k} - \kappa)^2}$

$$\mathcal{K}_{\text{virt}}(\mathbf{k}, \kappa) = 2 \epsilon(-\mathbf{k}^2) \delta^2(\mathbf{k} - \kappa)$$

$$\mathcal{K}_{\text{real}}(\mathbf{k}, \kappa) = \frac{N_c \alpha_s}{\pi^2} \frac{1}{(\mathbf{k} - \kappa)^2}$$

Solution for zero momentum transfer

Let us write symbolically:

$$\omega F = \mathbb{1} + \mathcal{K} \otimes F$$

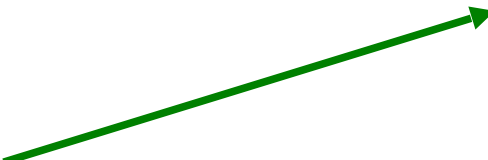
By solving the equation we mean finding eigenfunctions such that:

$$\mathcal{K} \otimes \phi_\alpha = \omega_\alpha \phi_\alpha$$

The eigenfunctions obey the completeness relation:

$$\sum_{\alpha} \phi_{\alpha}(\mathbf{k}) \phi_{\alpha}^*(\mathbf{k}') = \delta^2(\mathbf{k} - \mathbf{k}')$$

Then the solution to the first equation will be:

$$F(\omega, \mathbf{k}, \mathbf{k}') = \sum_{\alpha} \frac{\phi_{\alpha}(\mathbf{k}) \phi_{\alpha}^*(\mathbf{k}')}{\omega - \omega_{\alpha}}$$


α denotes a set of indices that can be discrete or continuous and the summation symbol can hide an integration

Solution for zero momentum transfer

Let us write symbolically:

$$\omega F = \mathbb{1} + \mathcal{K} \otimes F$$

By solving the equation we mean finding eigenfunctions such that:

$$\mathcal{K} \otimes \phi_\alpha = \omega_\alpha \phi_\alpha$$

Actually, if we use polar coordinates

$$\mathbf{k} \equiv (|\mathbf{k}|, \vartheta)$$

the eigenfunctions are:

$$\phi_{n\nu}(|\mathbf{k}|, \vartheta) = \frac{1}{\pi\sqrt{2}} (\mathbf{k}^2)^{-\frac{1}{2}+i\nu} e^{in\vartheta}$$

obeying:

$$\int d^2\mathbf{k} \phi_{n\nu}(\mathbf{k}) \phi_{n'\nu'}(\mathbf{k}) = \delta_{nn'} \delta(\nu - \nu')$$

whereas the eigenvalues are:

$$\omega_n(\nu) = -\frac{2\alpha_s N_c}{\pi} \operatorname{Re} \left[\psi \left(\frac{|n|+1}{2} + i\nu \right) - \psi(1) \right]$$

Solution for zero momentum transfer

The solution will then be:

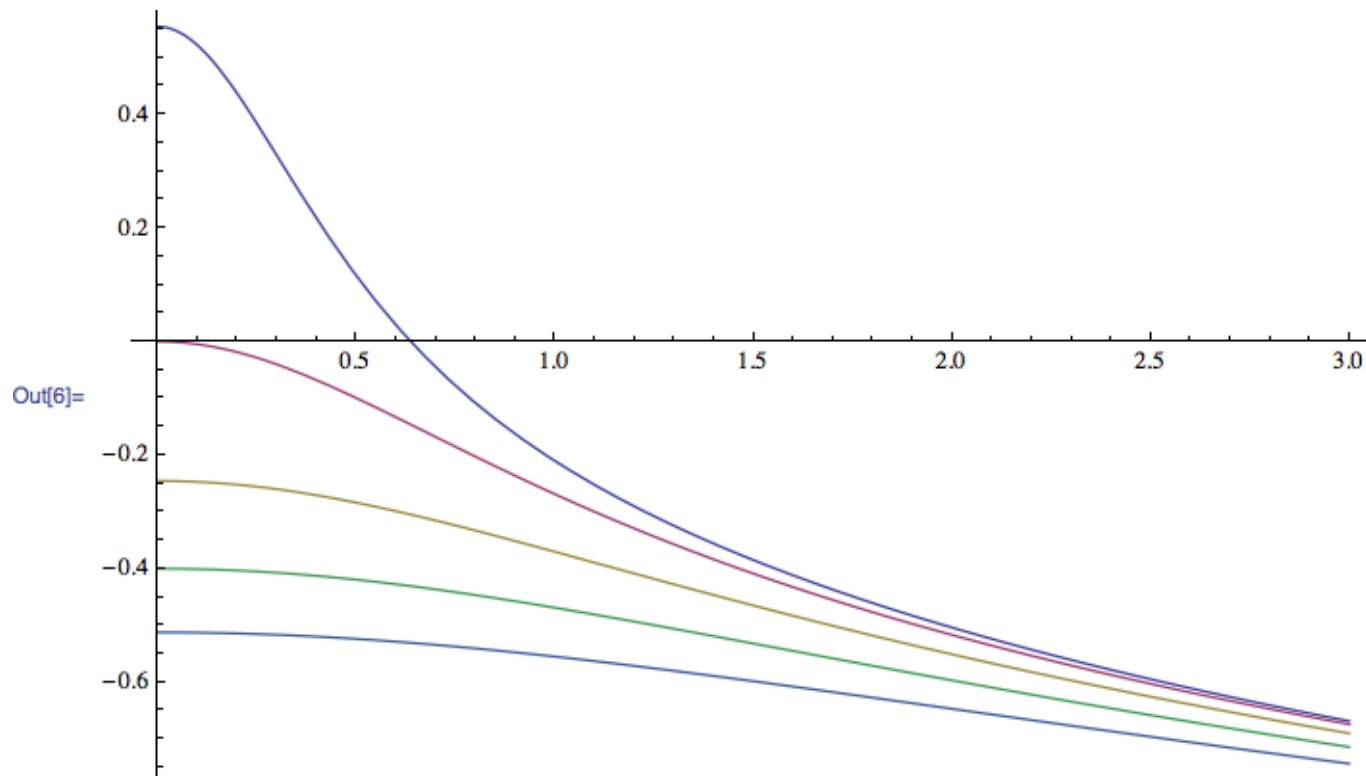
$$F(\omega, \mathbf{k}, \mathbf{k}') = \frac{1}{2\pi^2 (\mathbf{k}^2 \mathbf{k}'^2)^{\frac{1}{2}}} \sum_{n=0}^{\infty} e^{in(\vartheta - \vartheta')} \int_{-\infty}^{+\infty} d\nu \frac{e^{i\nu \ln\left(\frac{\mathbf{k}^2}{\mathbf{k}'^2}\right)}}{\omega - \omega_n(\nu)}$$

Here, n is also called conformal spin, it is connected to the angular information encoded in the gluon Green's function $F(\omega, \mathbf{k}, \mathbf{k}')$.

Solution for zero momentum transfer

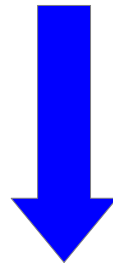
Let us use Mathematica to plot

```
omega[n_, v_] := Module[{asBar = 1/5},  
  Return[2 asBar (PolyGamma[0, 1] -  
    Re[PolyGamma[(Abs[n] + 1)/2 + I v]])];  
Plot[{omega[0, v], omega[1, v], omega[2, v],  
  omega[3, v], omega[4, v]}, {v, 0, 3}]
```



Solution for zero momentum transfer

$$F(\omega, \mathbf{k}, \mathbf{k}') = \frac{1}{2\pi^2 (\mathbf{k}^2 \mathbf{k}'^2)^{\frac{1}{2}}} \sum_{n=0}^{\infty} e^{in(\vartheta - \vartheta')} \int_{-\infty}^{+\infty} d\nu \frac{e^{i\nu \ln\left(\frac{\mathbf{k}^2}{\mathbf{k}'^2}\right)}}{\omega - \omega_n(\nu)}$$



Retain only the $n=0$ term, this from the analysis before

$$F(\omega, \mathbf{k}, \mathbf{k}') = \frac{1}{2\pi^2 (\mathbf{k}^2 \mathbf{k}'^2)^{\frac{1}{2}}} \int_{-\infty}^{+\infty} d\nu \frac{e^{i\nu \ln\left(\frac{\mathbf{k}^2}{\mathbf{k}'^2}\right)}}{\omega - \omega_0(\nu)}$$

Expanding around zero where we have the maximum gives:

$$\omega_0(\nu) = \frac{N_c \alpha_s}{\pi} (4 \ln 2 - 14 \zeta(3) \nu^2 + \dots)$$

Solution for zero momentum transfer

$$\omega_0(\nu) = \frac{N_c \alpha_s}{\pi} (4 \ln 2 - 14 \zeta(3) \nu^2 + \dots)$$

Set: $\lambda = \frac{N_c \alpha_s}{\pi} 4 \ln 2$, $\lambda' = \frac{N_c \alpha_s}{\pi} 28 \zeta(3)$

Take the inverse Mellin transform

$$F(s, \mathbf{k}, \mathbf{k}') = \frac{1}{2\pi^2 (\mathbf{k}^2 \mathbf{k}'^2)^{\frac{1}{2}}} \int_{-\infty}^{+\infty} d\nu \left(\frac{s}{\mathbf{k}^2}\right)^{\omega_0(\nu)} e^{i\nu \ln\left(\frac{\mathbf{k}^2}{\mathbf{k}'^2}\right)}$$

$$F(s, \mathbf{k}, \mathbf{k}') = \frac{1}{\sqrt{2\pi^3 \lambda' \mathbf{k}^2 \mathbf{k}'^2}} \frac{1}{\sqrt{\ln(s/\mathbf{k}^2)}} \times \left(\frac{s}{\mathbf{k}^2}\right)^\lambda \exp\left[-\frac{\ln^2(\mathbf{k}^2/\mathbf{k}'^2)}{2\lambda' \ln(s/\mathbf{k}^2)}\right]$$

Pomeron solution
of the BFKL
equation

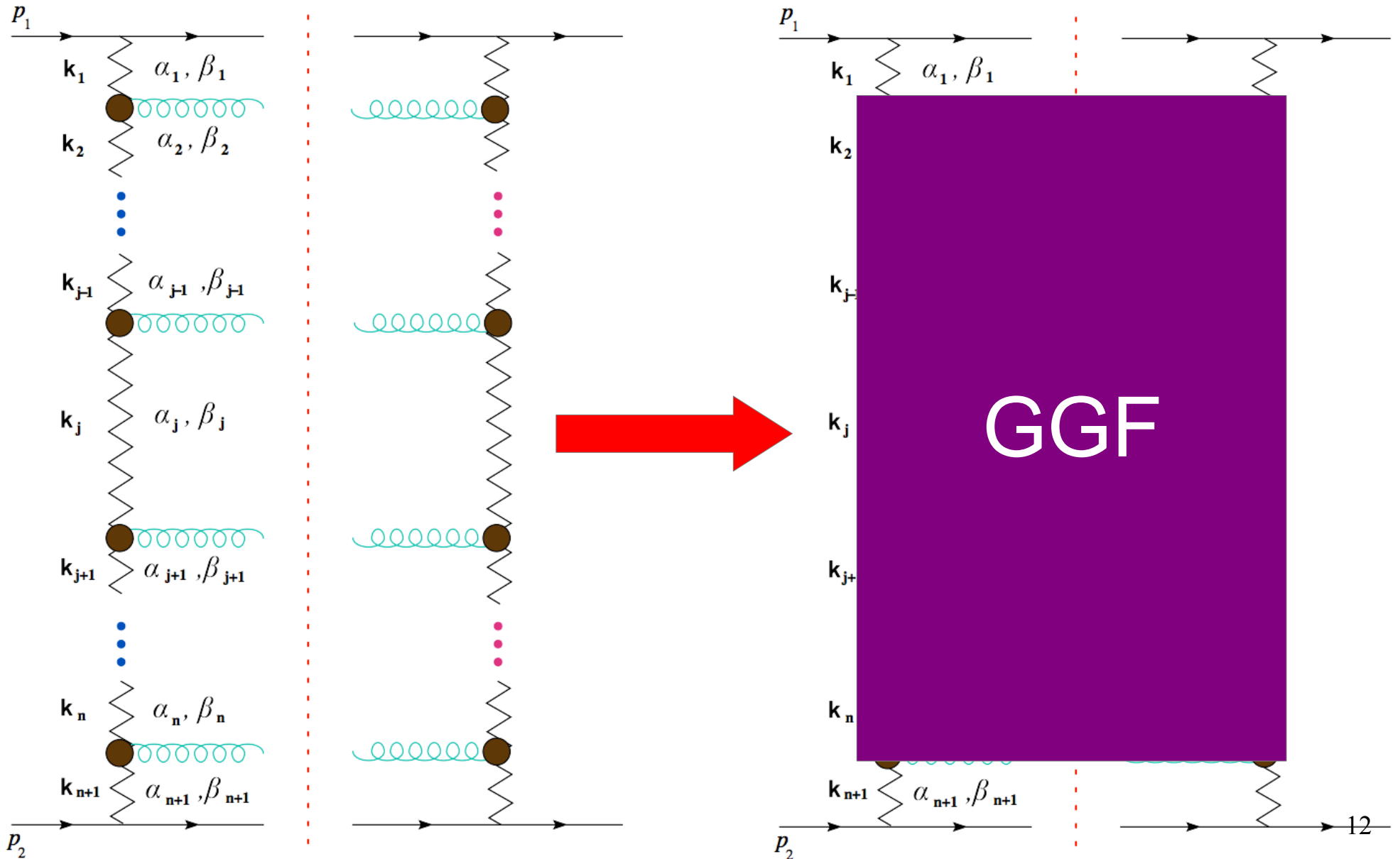
Solution for zero momentum transfer

$$F(s, \mathbf{k}, \mathbf{k}') = \frac{1}{\sqrt{2\pi^3 \lambda' \mathbf{k}^2 \mathbf{k}'^2}} \frac{1}{\sqrt{\ln(s/\mathbf{k}^2)}} \\ \times \left(\frac{s}{\mathbf{k}^2}\right)^\lambda \exp \left[-\frac{\ln^2(\mathbf{k}^2/\mathbf{k}'^2)}{2\lambda' \ln(s/\mathbf{k}^2)} \right]$$

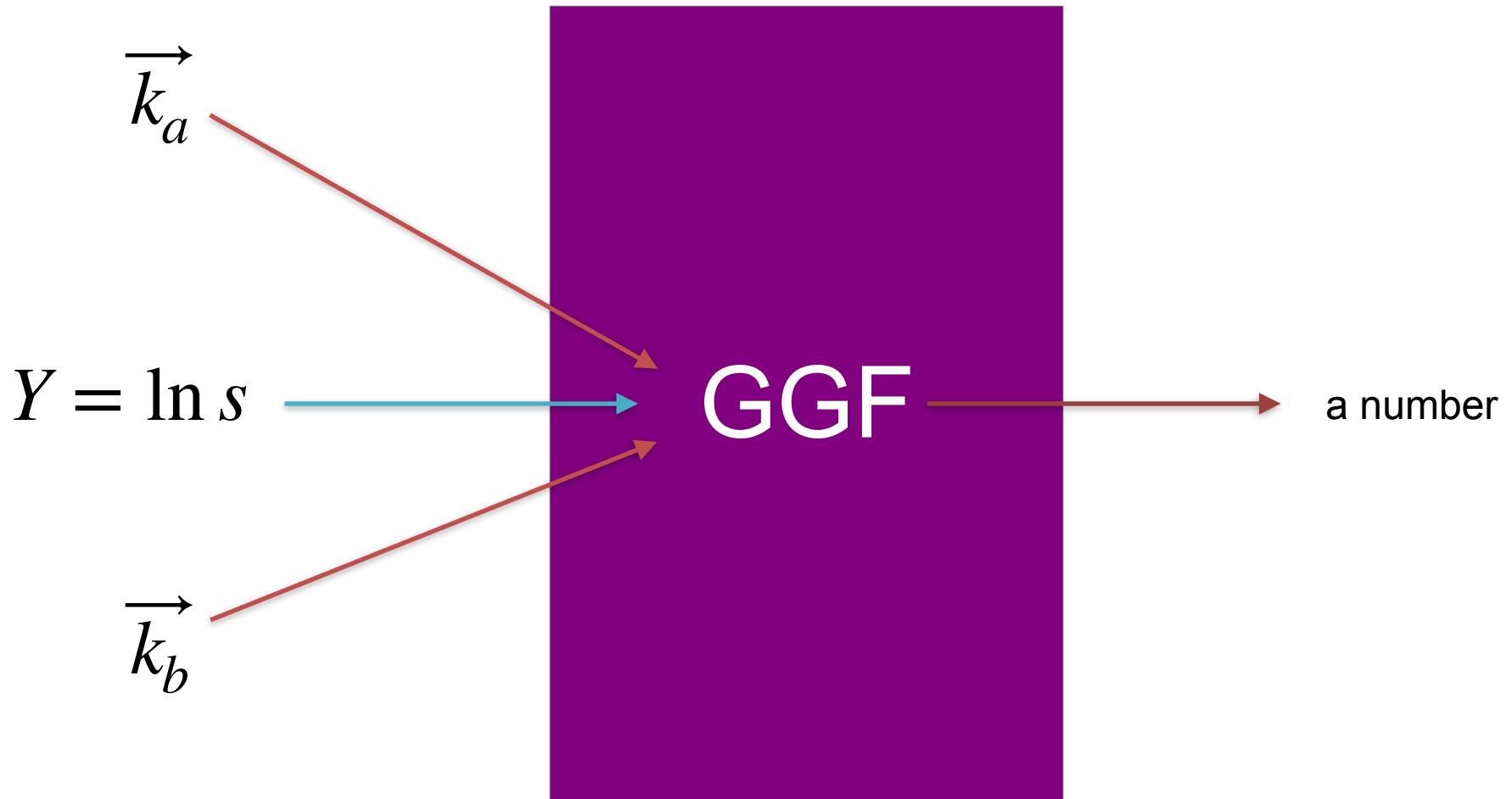
$$\alpha_{IP}(0) = 1 + \lambda = 1 + \frac{N_c \alpha_s}{\pi} 4 \ln 2$$

QCD Pomeron intercept way too large in comparison to the soft Pomeron intercept
If $a_s = 0.2$, the intercept is ~ 0.5

The gluon Green's function



Gluon Green's Function



Solution for zero momentum transfer

Again in Mathematica:

```
omega[n_, v_] := Module[{asBar = 1/5},  
  Return[2 asBar (PolyGamma[0, 1] -  
    Re[PolyGamma[(Abs[n] + 1)/2 + I v]])];
```

```
GGF[n_, Y_, ka_, kb_, angle_] :=  
NIntegrate[Exp[I*n*angle]/(2Pi^2)/ka/kb*2*Exp[omega[n,v]Y]*  
Cos[2 Log[(ka/kb)] v], {v, 0, Infinity}, WorkingPrecision -> 20];
```

Now you can calculate the LO gluon Green's function for a given rapidity Y , conformal spin n , and certain momenta of the reggeized gluons.

Note: Many times, in the literature, the leading eigenvalue is denoted as χ_0 . It is also sometimes called as the LO BFKL kernel!

$$\chi_0(\nu) = -2 \operatorname{Re} \left\{ \psi \left(\frac{1}{2} + i\nu \right) - \psi(1) \right\}$$

Solution for non-zero momentum transfer

$$f(k_a, k_b, q, Y) = \sum_{n=-\infty}^{\infty} \int_{-\infty}^{\infty} d\nu \mathcal{M}^{(n,\nu)}(k_a, q, Y) (\mathcal{M}^{(n,\nu)}(k_b, q, Y))^*$$

$$\begin{aligned} \mathcal{M}^{(n,\nu)}(k_a, q, Y) &= e^{Y\tilde{\omega}(\nu,n)} \frac{\sqrt{\mathcal{P}^{(n,\nu)}}}{2\pi^2 |k_a|^3} \left(\left(\frac{k_a^* q}{k_a q^*} \right)^{\frac{n}{2}} \left(\frac{|q|}{4|k_a|} \right)^{2i\nu} \right. \\ &\times \frac{\Gamma\left(\frac{3+n}{2} + i\nu\right)}{\Gamma\left(\frac{2+n}{2} + i\nu\right)} {}_2F_1\left(\frac{3+n}{2} + i\nu, \frac{1+n}{2} + i\nu; 1+n+i2\nu; \frac{q}{k_a}\right) \\ &\times \left. \frac{\Gamma\left(\frac{3-n}{2} + i\nu\right)}{\Gamma\left(\frac{2-n}{2} + i\nu\right)} {}_2F_1\left(\frac{3-n}{2} + i\nu, \frac{1-n}{2} + i\nu; 1-n+i2\nu; \frac{q^*}{k_a^*}\right) - \text{c.c.} \right) \end{aligned}$$

$$\begin{aligned} \mathcal{P}^{(n,\nu)} &= \frac{((-1)^n + \cosh(2\pi\nu)) |\Gamma\left(\frac{2+n}{2} + i\nu\right) \Gamma\left(\frac{2-n}{2} + i\nu\right)|^2}{2\left(\nu^2 + \left(\frac{n+1}{2}\right)^2\right) \left(\nu^2 + \left(\frac{n-1}{2}\right)^2\right)} \\ &= \pi^2 \frac{|\Gamma\left(\frac{2+n}{2} + i\nu\right) \Gamma\left(\frac{2-n}{2} + i\nu\right)|^2}{|\Gamma\left(\frac{3+n}{2} + i\nu\right) \Gamma\left(\frac{3-n}{2} + i\nu\right)|^2} \end{aligned}$$

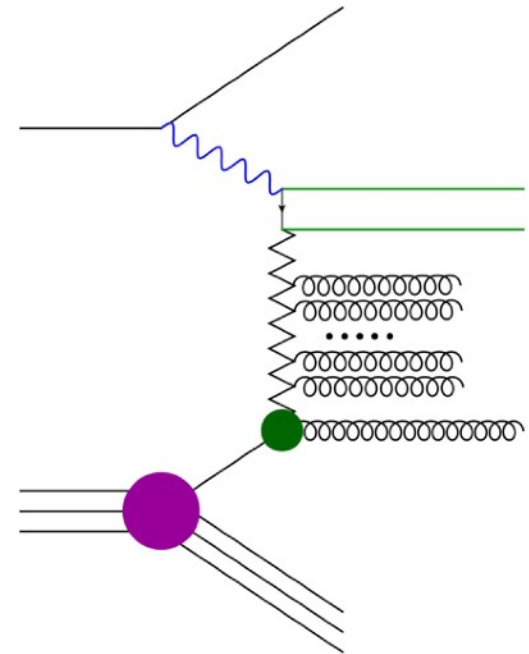
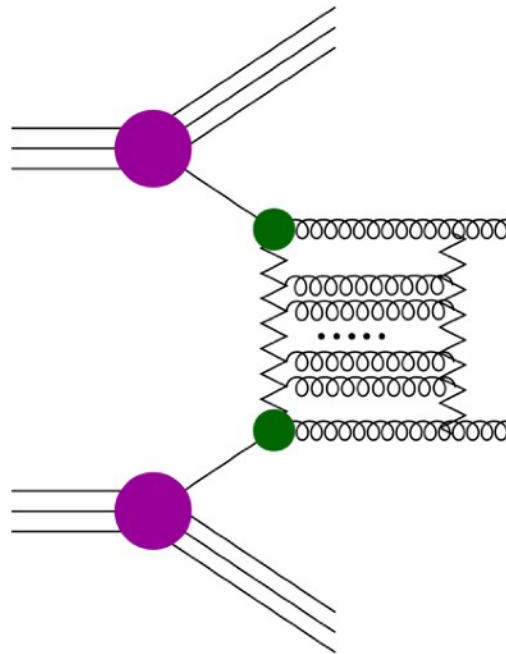
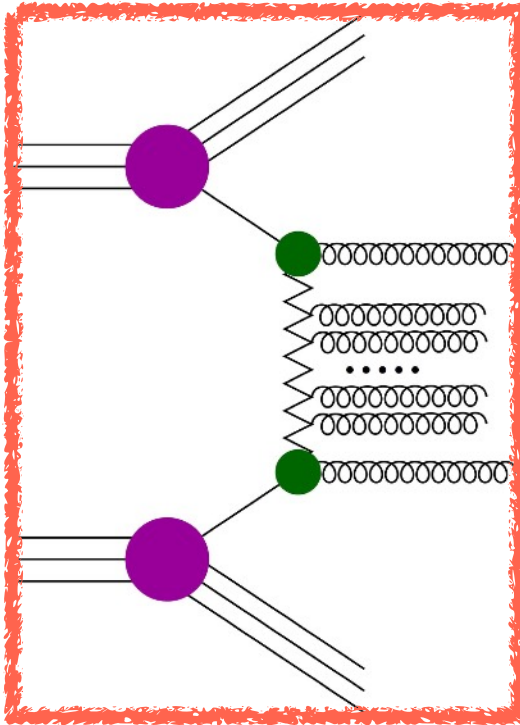
High energy scattering QCD

multi-Regge kinematics at colliders

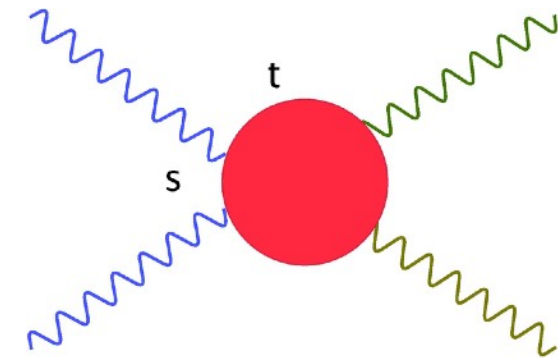
Mueller-Navelet (MN) jets

rapidity gaps

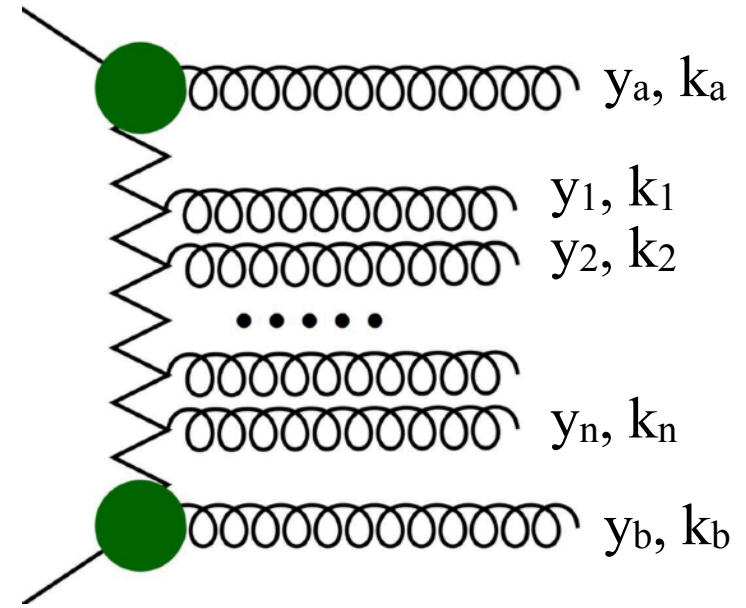
DIS



The high energy or *Regge* limit



$$s \gg -t \gg m^2$$



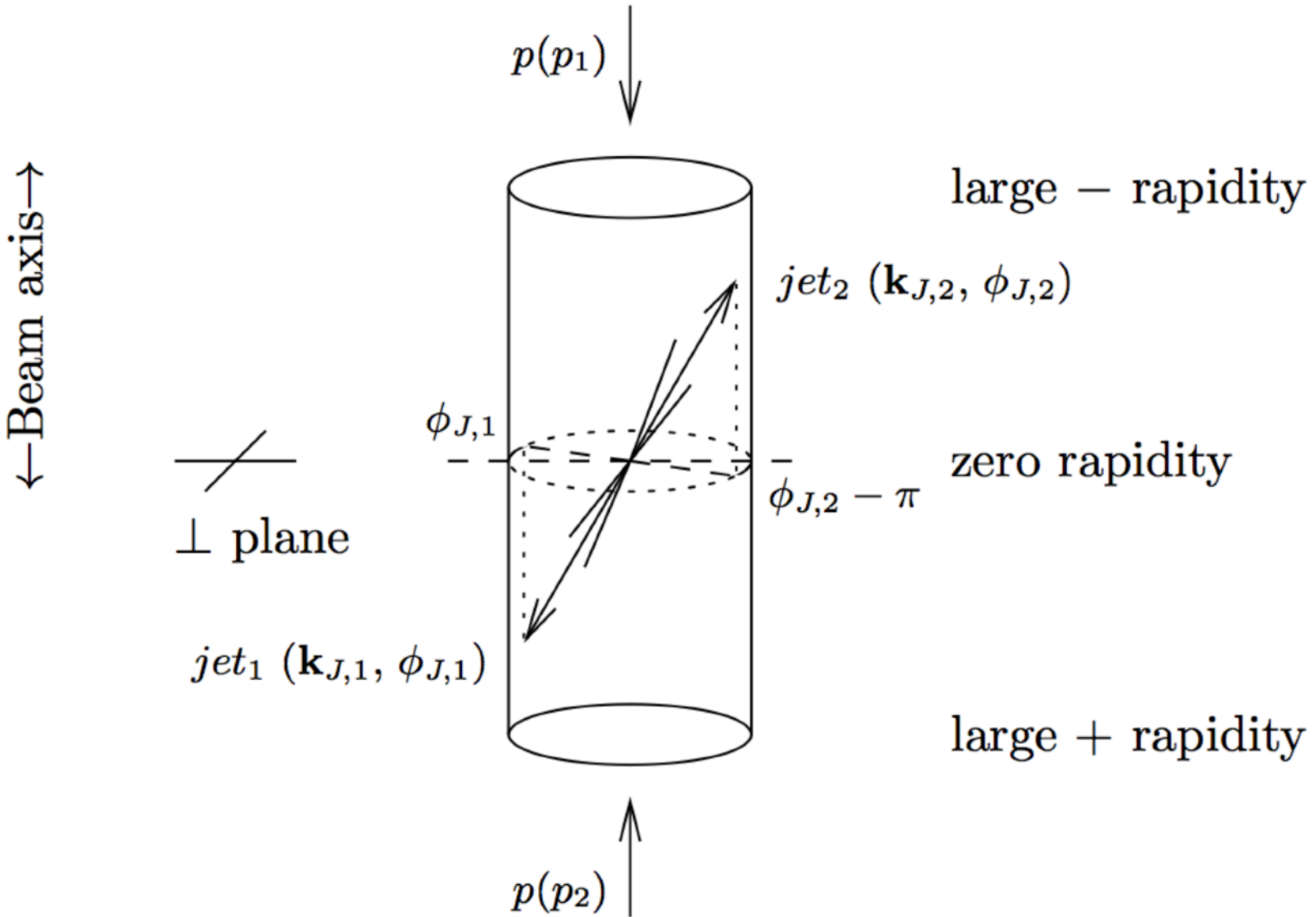
$$y_b \ll y_n \ll \dots \ll y_2 \ll y_1 \ll y_a$$

$$|k_{b\perp}| \simeq |k_{n\perp}| \simeq \dots \simeq |k_{2\perp}| \simeq |k_{1\perp}| \simeq |k_{a\perp}|$$

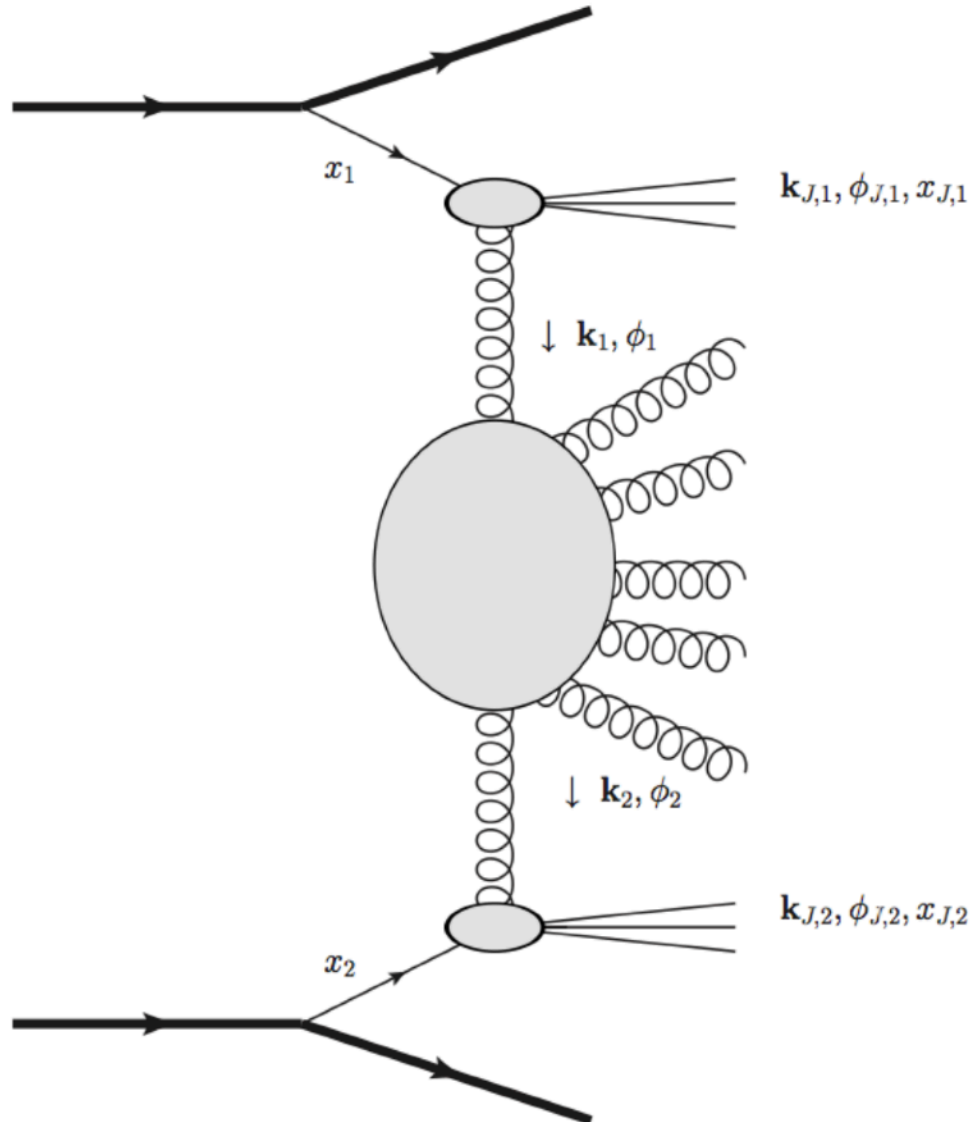
$n+2$ particle production in multi-Regge kinematics:

- strong ordering in rapidity
- similar transverse momenta
- Use *Balitsky-Fadin-Kuraev-Lipatov* (BFKL) dynamics. BFKL resums to all orders diagrams that carry **large logarithms** in energy.

Mueller-Navelet jets



Mueller-Navelet jets



Mueller-Navelet jets

$$p(p_1) + p(p_2) \rightarrow \text{jet}(k_{J_1}) + \text{jet}(k_{J_2}) + X$$

$$k_{J_1} = x_{J_1} p_1 + \frac{\vec{k}_{J_1}^2}{x_{J_1} s} p_2 + k_{J_1 \perp}, \quad k_{J_1 \perp}^2 = -\vec{k}_{J_1}^2$$

$$k_{J_2} = x_{J_2} p_2 + \frac{\vec{k}_{J_2}^2}{x_{J_2} s} p_1 + k_{J_2 \perp}, \quad k_{J_2 \perp}^2 = -\vec{k}_{J_2}^2$$

$$y_1 = \frac{1}{2} \ln \frac{x_{J_1}^2 s}{\vec{k}_{J_1}^2}, \quad dy_1 = \frac{dx_{J_1}}{x_{J_1}},$$

$$y_2 = -\frac{1}{2} \ln \frac{x_{J_2}^2 s}{\vec{k}_{J_2}^2}, \quad dy_2 = -\frac{dx_{J_2}}{x_{J_2}}$$

$$\Delta y \equiv Y = \ln \frac{x_{J_1} x_{J_2} s}{|\vec{k}_{J_1}| |\vec{k}_{J_2}|}$$

Mueller-Navelet jets

$$p(p_1) + p(p_2) \rightarrow \text{jet}(k_{J_1}) + \text{jet}(k_{J_2}) + X$$

$$\frac{d\sigma}{dx_{J_1} dx_{J_2} d^2k_{J_1} d^2k_{J_2}} = \sum_{i,j=q,\bar{q},g} \int_0^1 dx_1 \int_0^1 dx_2 f_i(x_1, \mu_F) f_j(x_2, \mu_F) \frac{d\hat{\sigma}_{i,j}(x_1 x_2 s, \mu_F)}{dx_{J_1} dx_{J_2} d^2k_{J_1} d^2k_{J_2}}$$

$$\frac{d\hat{\sigma}_{i,j}(x_1 x_2 s)}{dx_{J_1} dx_{J_2} d^2k_{J_1} d^2k_{J_2}} = \frac{1}{(2\pi)^2} \int \frac{d^2q_1}{\vec{q}_1^2} V_i(\vec{q}_1, s_0, x_1; \vec{k}_{J_1}, x_{J_1}) \int \frac{d^2q_2}{\vec{q}_2^2} V_j(-\vec{q}_2, s_0, x_2; \vec{k}_{J_2}, x_{J_2})$$

$$\times \int_{\delta-i\infty}^{\delta+i\infty} \frac{d\omega}{2\pi i} \left(\frac{x_1 x_2 s}{s_0} \right)^\omega G_\omega(\vec{q}_1, \vec{q}_2).$$

GGF (Mathematica)

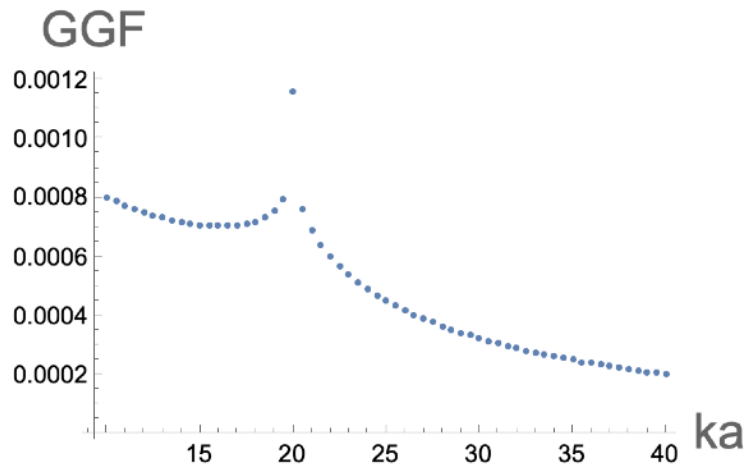
```
asBar = 1 / 5;
```

```
omega[n_, v_] :=  
  Block[{}],  
  Return[  
    2 asBar (PolyGamma[0, 1] - Re[PolyGamma[(Abs[n] + 1) / 2 + I v]])]];
```

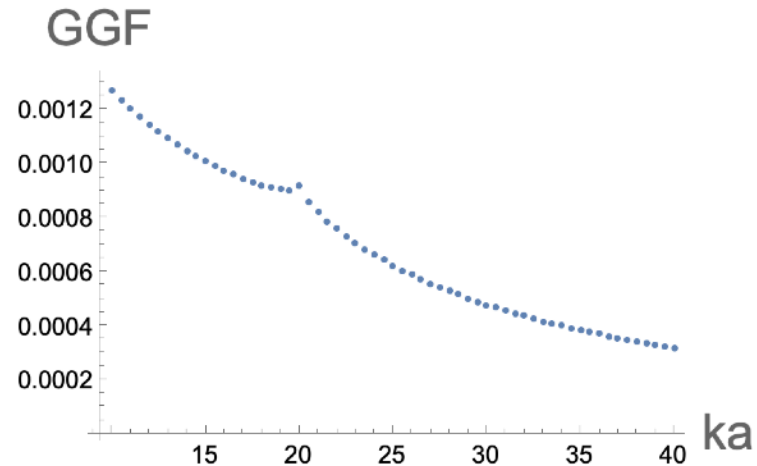
```
GGF[n_, Y_, ka_, kb_, angle_] :=  
  NIntegrate[Exp[I n angle] / (2 Pi ^ 2) / ka / kb ^ 2 Exp[omega[n, v] Y] *  
    Cos[2 Log[(ka / kb)] v], {v, 0, Infinity},  
  Method -> "DoubleExponentialOscillatory", WorkingPrecision -> 20,  
  PrecisionGoal -> 10, MaxRecursion -> 20];
```

GGF (Mathematica)

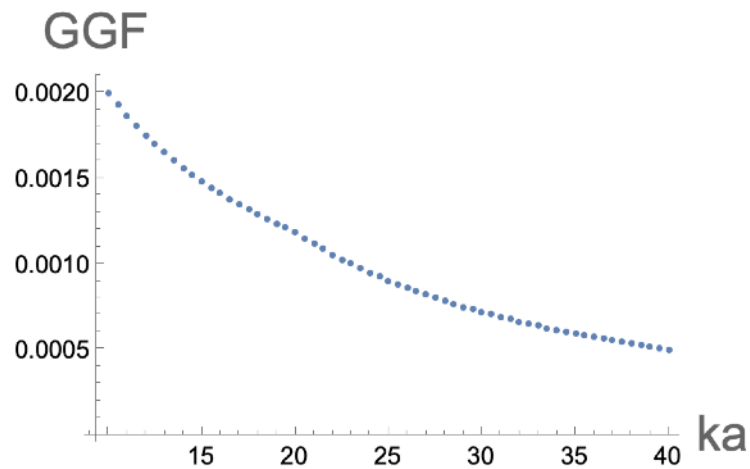
```
Table[{ka, GGF[0, 3, ka, 20, 0]}, {ka, 10, 40, 1/2}];  
ListPlot[%, AxesLabel -> {Style[ka, Large], Style[GGF, Large]},  
AxesStyle -> Directive[12]]
```



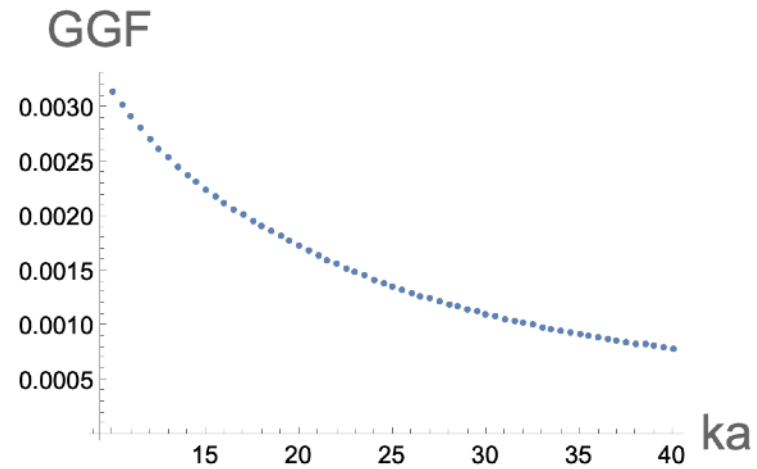
```
Table[{ka, GGF[0, 4, ka, 20, 0]}, {ka, 10, 40, 1/2}];  
ListPlot[%, AxesLabel -> {Style[ka, Large], Style[GGF, Large]},  
AxesStyle -> Directive[12]]
```

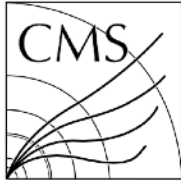


```
Table[{ka, GGF[0, 5, ka, 20, 0]}, {ka, 10, 40, 1/2}];  
ListPlot[%, AxesLabel -> {Style[ka, Large], Style[GGF, Large]},  
AxesStyle -> Directive[12]]
```



```
Table[{ka, GGF[0, 6, ka, 20, 0]}, {ka, 10, 40, 1/2}];  
ListPlot[%, AxesLabel -> {Style[ka, Large], Style[GGF, Large]},  
AxesStyle -> Directive[12]]
```





CMS-FSQ-12-002



CERN-PH-EP/2015-309
2016/01/26

Azimuthal decorrelation of jets widely separated in rapidity in pp collisions at $\sqrt{s} = 7$ TeV

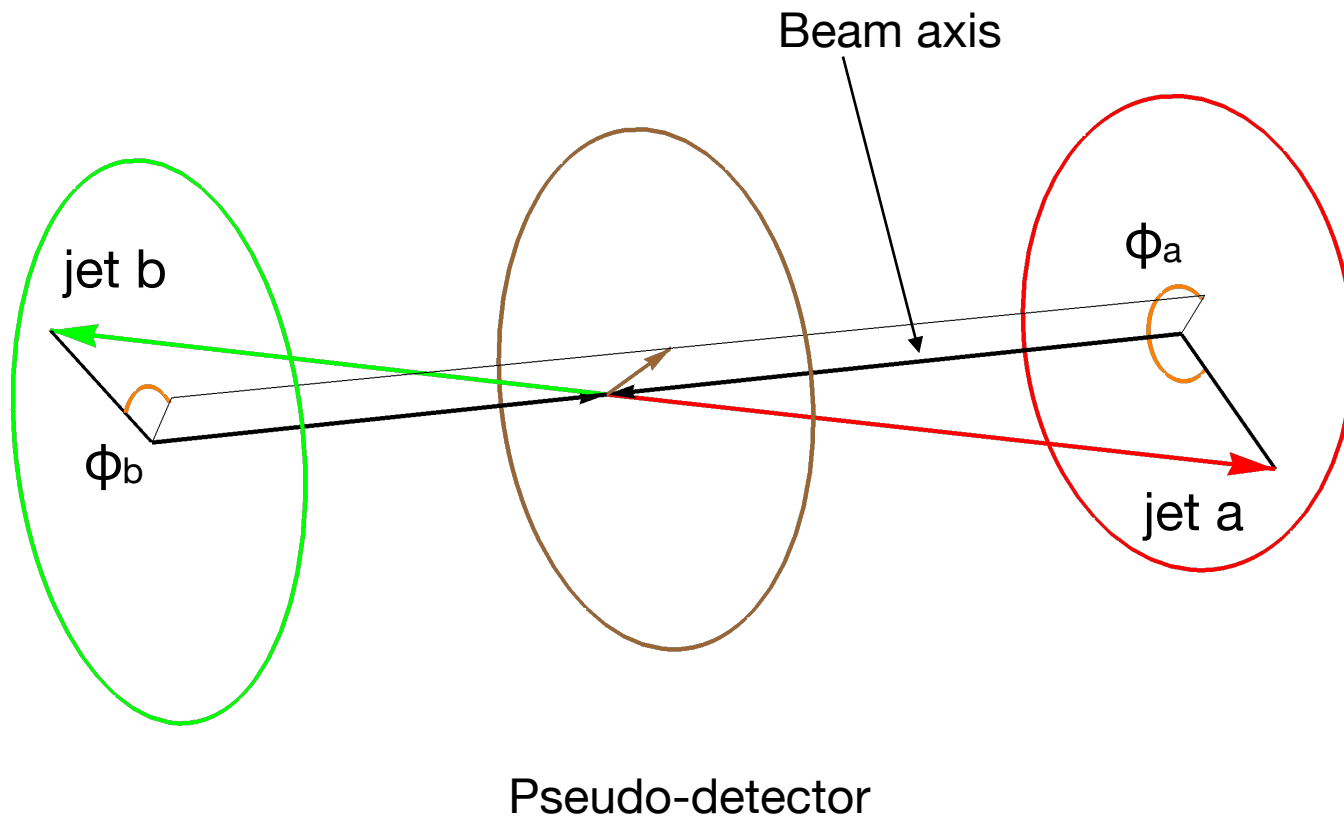
The CMS Collaboration*

Key question: What is the applicability energy window for BFKL? Is it at LHC energies?

In the Conclusions of that paper, it reads:

The observed sensitivity to the implementation of the colour-coherence effects in the DGLAP MC generators and the reasonable data-theory agreement shown by the NLL BFKL analytical calculations at large Δy , may be considered as indications that the kinematical domain of the present study lies in between the regions described by the DGLAP and BFKL approaches. Possible manifestations of BFKL signatures are expected to be more pronounced at increasing collision energies.

A MN jets example with an extra central jet tagged



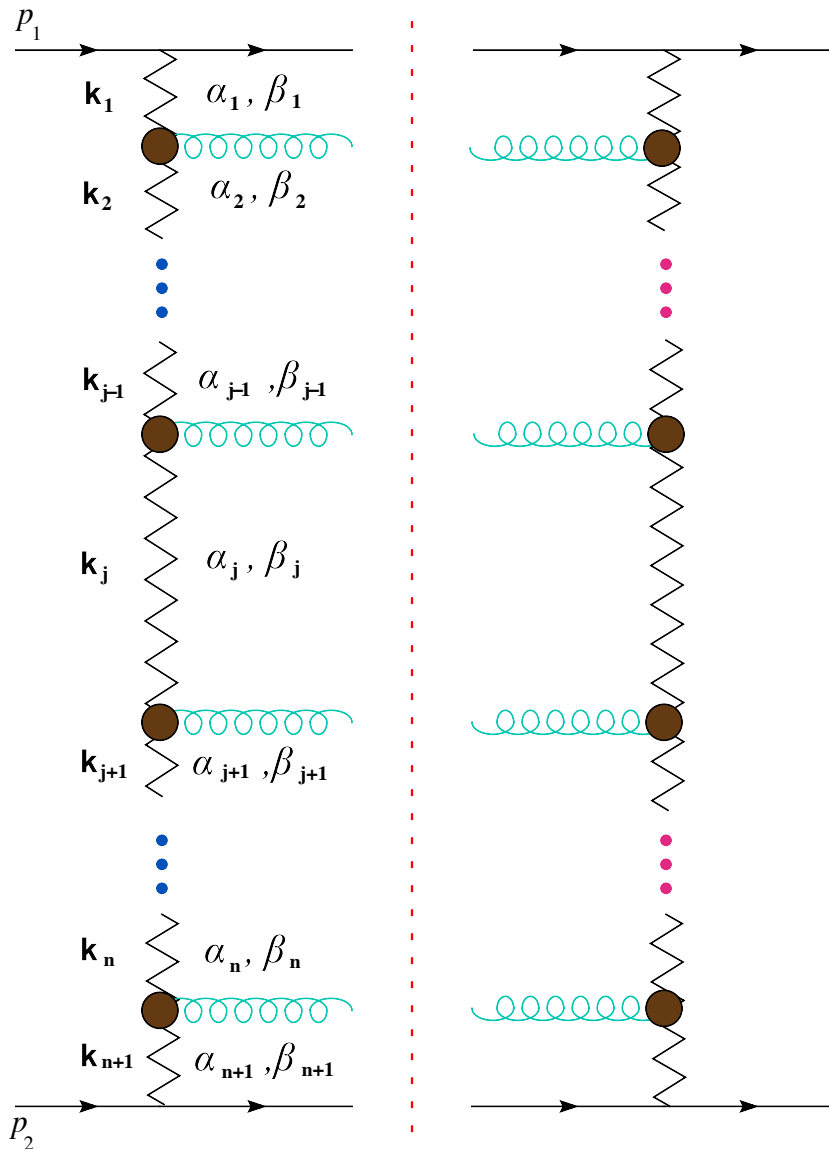
BFKLex

- A Monte Carlo code for the iterative solution of the BFKL equation
- The big advantage of a MC code is that differential information regarding the rapidities and momenta of the final state gluons can be booked and differential distributions for a large number of observables can be produced.
- Already, BFKLex was used to propose new observables in order to search for BFKL related effects at the LHC.
- We can run the code to compute the gluon Green's function omitting the bounding jets, PDFs, impact factors etc. (partonic level)
- We can run the code including all the omissions of the previous step (full-run)

Why a Monte Carlo approach?

- We don't always know the analytic solution
- Even if we know it, we still want to store and analyze information about “differential” quantities (e.g. rapidities, transverse momenta, angles) that will be lost once we perform the integrations analytically. We want this for two reasons:
 1. Because then we can compare theoretical predictions to a greater set of observables
 2. Because there are lots of things we can still learn about concepts we use every day and maybe we don't fully understand
- We want to have a common language with people that work and are familiar with fixed order calculations and who are the majority in the “pheno” community – the interaction will help both sides
- We want to work in momentum space
- Connect to Heavy Ion physics
- Connect to physics of Cosmic Rays

Large logs from real emission corrections in a Monte Carlo setup



- Assume Reggeons in the t-channel
- Assume you have only one real emission
- Do the phase-space integration \rightarrow res1
- Now assume you have two real emissions
- Do the phase-space integration \rightarrow res2
- Add the results: RES = res1+res2
- Now assume you have three real emissions
- Do the phase-space integration \rightarrow res3
- Add the results: RES = RES + res3
- Repeat until you have N real emissions with resN so tiny compared to RES such that you are allowed to claim convergence

NOTE: The phase-space integration is over rapidity and transverse momenta.

BFKLex, a BFKL Monte Carlo

- The main goal was to have a tool that calculates the gluon Green's function (GGF) and other differential observables.
- The GGF is the solution to the BFKL equation. Use the iterative form:

$$f = e^{\omega(\vec{k}_A)Y} \left\{ \delta^{(2)}(\vec{k}_A - \vec{k}_B) + \sum_{n=1}^{\infty} \prod_{i=1}^n \frac{\alpha_s N_c}{\pi} \int d^2 \vec{k}_i \frac{\theta(k_i^2 - \lambda^2)}{\pi k_i^2} \right. \\ \left. \int_0^{y_i-1} dy_i e^{(\omega(\vec{k}_A + \sum_{l=1}^i \vec{k}_l) - \omega(\vec{k}_A + \sum_{l=1}^{i-1} \vec{k}_l))y_i} \delta^{(2)}\left(\vec{k}_A + \sum_{l=1}^n \vec{k}_l - \vec{k}_B\right) \right\}$$

$\omega(\vec{q}) = -\frac{\alpha_s N_c}{\pi} \log \frac{q^2}{\lambda^2}$ is the gluon Regge trajectory

The implementation of the **BFKLex** is in C++, G.C & A. Sabio Vera

Some results with BFKLex

A Comparative study of small x Monte Carlos with and without QCD coherence effects

G. C, M. Deak, A.Sabio Vera, P. Stephens

Nucl.Phys. B849 (2011) 28-44

The Colour Octet Representation of the Non-Forward BFKL Green Function

G. C, A. Sabio Vera.

Phys.Lett. B709 (2012) 301-308

The NLO $N = 4$ SUSY BFKL Green function in the adjoint representation

G. C, A.Sabio Vera

Phys.Lett. B717 (2012) 458-461

Bootstrap and momentum transfer dependence in small x evolution equations

G. C, A. Sabio Vera, C. Salas

Phys.Rev. D87 (2013) no.1, 016007

A study of the diffusion pattern in $N = 4$ SYM at high energies

F. Caporale, G. C, J.D. Madrigal, B. Murdaca, A. Sabio Vera

Phys.Lett. B724 (2013) 127-132

Monte Carlo study of double logarithms in the small x region

G. C, A. Sabio Vera

Phys.Rev. D93 (2016) no.7, 074004

The high-energy radiation pattern from BFKLex with double-log collinear contributions

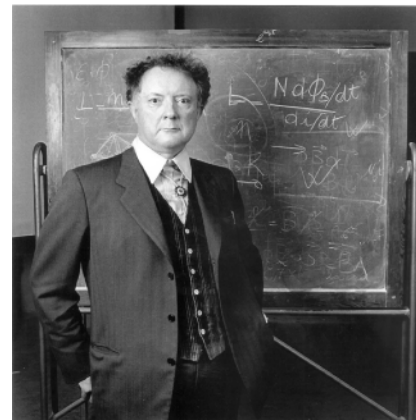
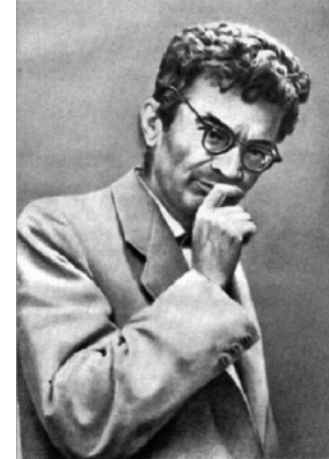
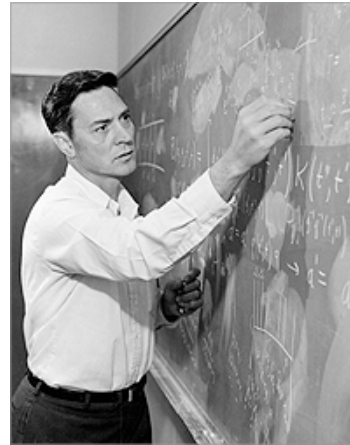
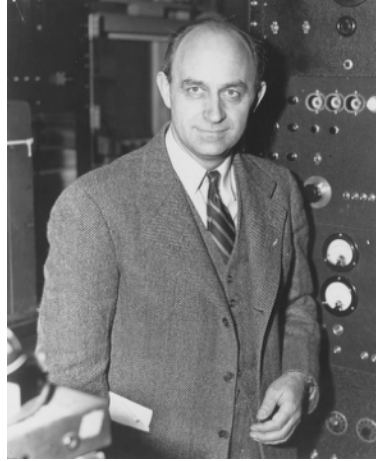
G. C, A. Sabio Vera

JHEP 1602 (2016) 064

Back to the past once more

- Multiparticle production 50-60 years ago
- The emergence of the so-called multiperipheral models and the concept of clusters in the 60s and 70s
- An important tool that comes from the past: two particle correlations
- How do these old ideas fare in the QCD era and are they useful at all?
- To answer that, go to a certain kinematical limit (multi-Regge kinematics) and use Monte Carlo techniques (**BFKL**ex)

... some of the leading figures those days



~70 years ago

Progress of Theoretical Physics, Vol. 5, No. 4, July~August, 1950

High Energy Nuclear Events

ENRICO FERMI

Institute for Nuclear Studies

University of Chicago

Chicago, Illinois

(Received June 30, 1950)

Abstract

A statistical method for computing high energy collisions of protons with multiple production of particles is discussed. The method consists in assuming that as a result of fairly strong interactions between nucleons and mesons the probabilities of formation of the various possible numbers of particles are determined essentially by the statistical weights of the various possibilities.

~50 years ago

CORRELATIONS AND MULTIPLICITY DISTRIBUTIONS IN MULTIPARTICLE PRODUCTION

BY M. LE BELLAC

University of Nice*

(Presented at the XIII Cracow School of Theoretical Physics, Zakopane, June 1-12, 1973)

A general discussion of Short Range Order hypothesis and its comparison with experimental data on correlations in inclusive spectra is given.

1. Introduction

In the absence of a theory of strong interactions, one of the main purposes of the present experiments on multiparticle production is to discover empirical regularities in the experimental data, in the hope that these regularities will be useful later for a more fundamental understanding of hadrodynamics. Some of these empirical regularities have

Chew, G. F., 'Multiperipheralism and the Bootstrap,'
Comments on Nuclear and Particle Physics 2 (1968),
163–168.

Multiperipheralism and the Bootstrap

The adjective “peripheral”, when applied to hadronic reactions, characterizes a correlation between large angular-momentum values that produces a smooth and persistent momentum-transfer dependence favoring small angles. The best-known example is the so called “forward diffraction peak” in elastic scattering, but almost all two-hadron reactions have exhibited similar forward peaking, with widths in momentum transfer that change only slowly with energy. The widths vary from one reaction to another but usually are well below 0.5 GeV. Although “peripheralism” at first sight may seem an unsurprising phenomenon, close study has revealed profound theoretical implications that touch on the very origin of the hadrons. One crucial inference is that multiple-production reactions should be “multiply-peripheral”.

This note proposes briefly to survey multiperipheralism, together with the related hypothesis of multi-Regge-poles. It will be seen that a new class of bootstrap constraints is implied.

Sergio Fubini
Comments Nucl.Part.Phys. 4 (1970) 3, 102-106

Multiperipheral Model

Work in the multiperipheral model was started almost ten years ago. It is pleasant to realize that the model in its different forms retains the attention of many physicists and that some of its general predictions seem to be in good agreement with experiment.¹

Although a detailed study of the model requires a rather involved mathematical apparatus, most of the main results can be understood in a simple intuitive way.

The multiperipheral model is based on the idea that multiple production at high energy is dominated by the graphs shown in Fig. 1.

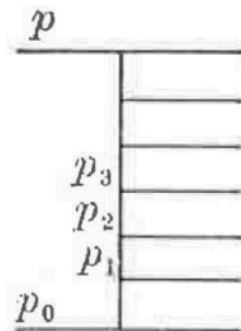


FIGURE 1

The different versions of the model differ in the choice of what object (particle, Regge poles ...) corresponds to the peripheral lines of momentum $p_1, p_2 \dots$.

Notion of Clusters (70s)

Progress of Theoretical Physics, Vol. 53, No. 3, March 1975

786

S. Matsuda, K. Sasaki and T. Uematsu

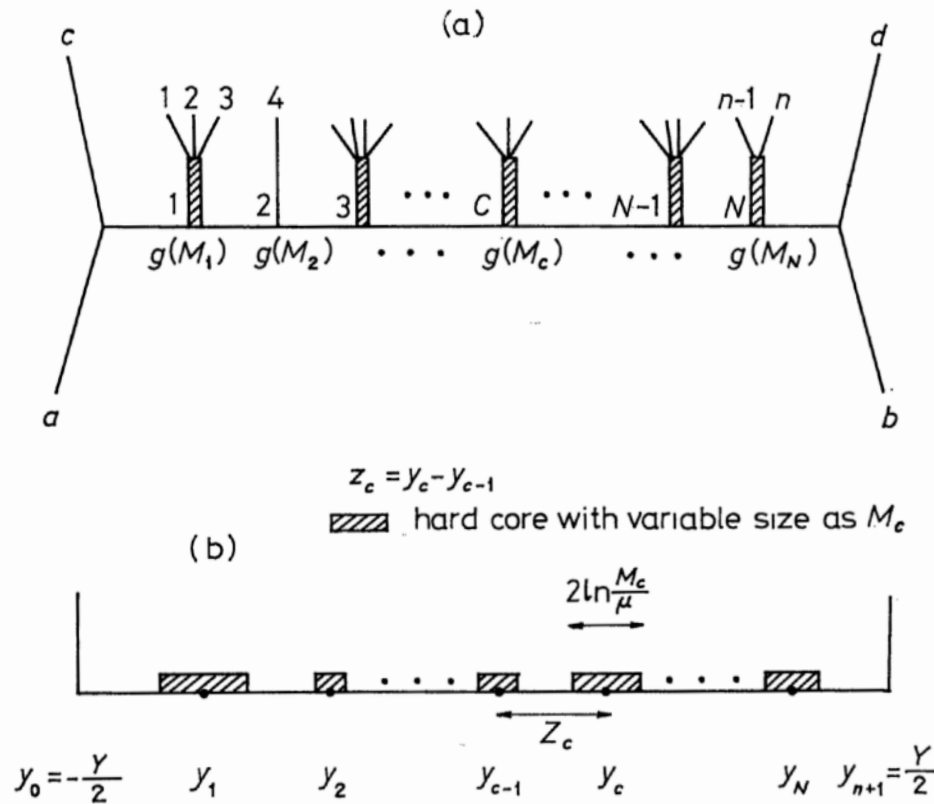


Fig. 1 (a) Multiperipheral chain of our cluster emission model. (b) Rapidity space configuration of clusters with variable mass M_c . Each cluster has a hard core of length $2 \ln(M_c/\mu)$.

High energy scattering at hadron colliders

- The first hadron collider was the 1-km-circumference proton–proton (pp) **Intersecting Storage Rings (ISR)**,¹ commissioned at CERN in 1971. Its beam energies ranged from 12 to 31 GeV. Experiments at the ISR revealed the logarithmic rise of the pp total scattering cross section at energies where it was expected to have levelled off.
- Ten years later, CERN's **Super Proton Synchrotron (SPS)**, until then a fixed-target accelerator, became the **SppS**, a proton–antiproton collider with E_{cm} up to 630 GeV. By the end of 1983, the collaborations that ran the large UA1 and UA2 detectors at the collider's beam-crossing points had **discovered the heavy W_{\pm} and Z^0** bosons that mediate the weak interactions
- Next, Fermilab's pp **Tevatron** collider had a E_{cm} of 1.8 TeV; eventually it reached 2 TeV. **1995 top quark discovery**
- Currently: **LHC** era

Multiperipheral models vs perturbative QCD

- The key idea is to **use** an old multiperipheral model, namely the **Chew-Pignotti model** (*Phys.Rev. 176 ,1968*) as used by DeTar (*Phys. Rev. D, 3 1971*) for **multi-jet final states at the LHC** assuming that the **jet multiplicity is fixed** and rather large and the total rapidity interval is large (similar to Mueller-Navelet jets).
- By jets in this context we really mean final state gluons before parton shower and before hadronization
- Produce **jet rapidity distributions** and **jet-jet rapidity correlations**
- We then want to produce the same distributions with **BFKLex** and compare the two approaches

A first comparison can be found in

Nucl.Phys.B 971 (2021) 115518, N. Bethencourt de León, GC and A. Sabio Vera

Definition of the two-particle rapidity-rapidity correlation function

$$C_2(y_1, p_{\perp 1}, y_2, p_{\perp 2}) = \frac{1}{\sigma_{in}} \frac{d^6 \sigma}{dy_1 d^2 p_{\perp 1} dy_2 d^2 p_{\perp 2}} - \frac{1}{\sigma_{in}^2} \frac{d^3 \sigma}{dy_1 d^2 p_{\perp 1}} \frac{d^3 \sigma}{dy_2 d^2 p_{\perp 2}}$$

We integrate over p_T

$$\rho_1(y) = \frac{1}{\sigma_{in}} \int d^2 p_{\perp} \frac{d^3 \sigma}{dy d^2 p_{\perp}}$$

$$\rho_2(y_1, y_2) = \frac{1}{\sigma_{in}} \int d^2 p_{\perp 1} d^2 p_{\perp 2} \frac{d^6 \sigma}{dy_1 d^2 p_{\perp 1} dy_2 d^2 p_{\perp 2}}$$

to get:

$$C_2(y_1, y_2) = \frac{1}{\sigma_{in}} \frac{d^2 \sigma}{dy_1 dy_2} - \frac{1}{\sigma_{in}^2} \frac{d\sigma}{dy_1} \frac{d\sigma}{dy_2} \equiv \rho_2(y_1, y_2) - \rho_1(y_1) \rho_1(y_2)$$

$$R_2(y_1, y_2) = \frac{C_2(y_1, y_2)}{\rho_1(y_1) \rho_1(y_2)} = \frac{\rho_2(y_1, y_2)}{\rho_1(y_1) \rho_1(y_2)} - 1$$

Signal
Background

Rapidity distributions in the Chew-Pignotti model

Single differential distribution

$$\frac{d\sigma_{N+2}^{(l)}}{dy_l} = \alpha^{N+2} \frac{\left(\frac{Y}{2} - y_l\right)^{N-l}}{(N-l)!} \frac{\left(y_l + \frac{Y}{2}\right)^{l-1}}{(l-1)!}$$

Double differential distribution

$$\frac{d^2\sigma_{N+2}^{(l,m)}}{dy_l dy_m} = \alpha^{N+2} \frac{\left(\frac{Y}{2} - y_l\right)^{N-l}}{(N-l)!} \frac{(y_l - y_m)^{l-m-1}}{(l-m-1)!} \frac{\left(y_m + \frac{Y}{2}\right)^{m-1}}{(m-1)!}$$

- The key point in the Chew-Pignotti model is that longitudinal and transverse degrees of freedom decouple.
- One of the standard ways to show double differential distributions and correlation functions is with contour plots

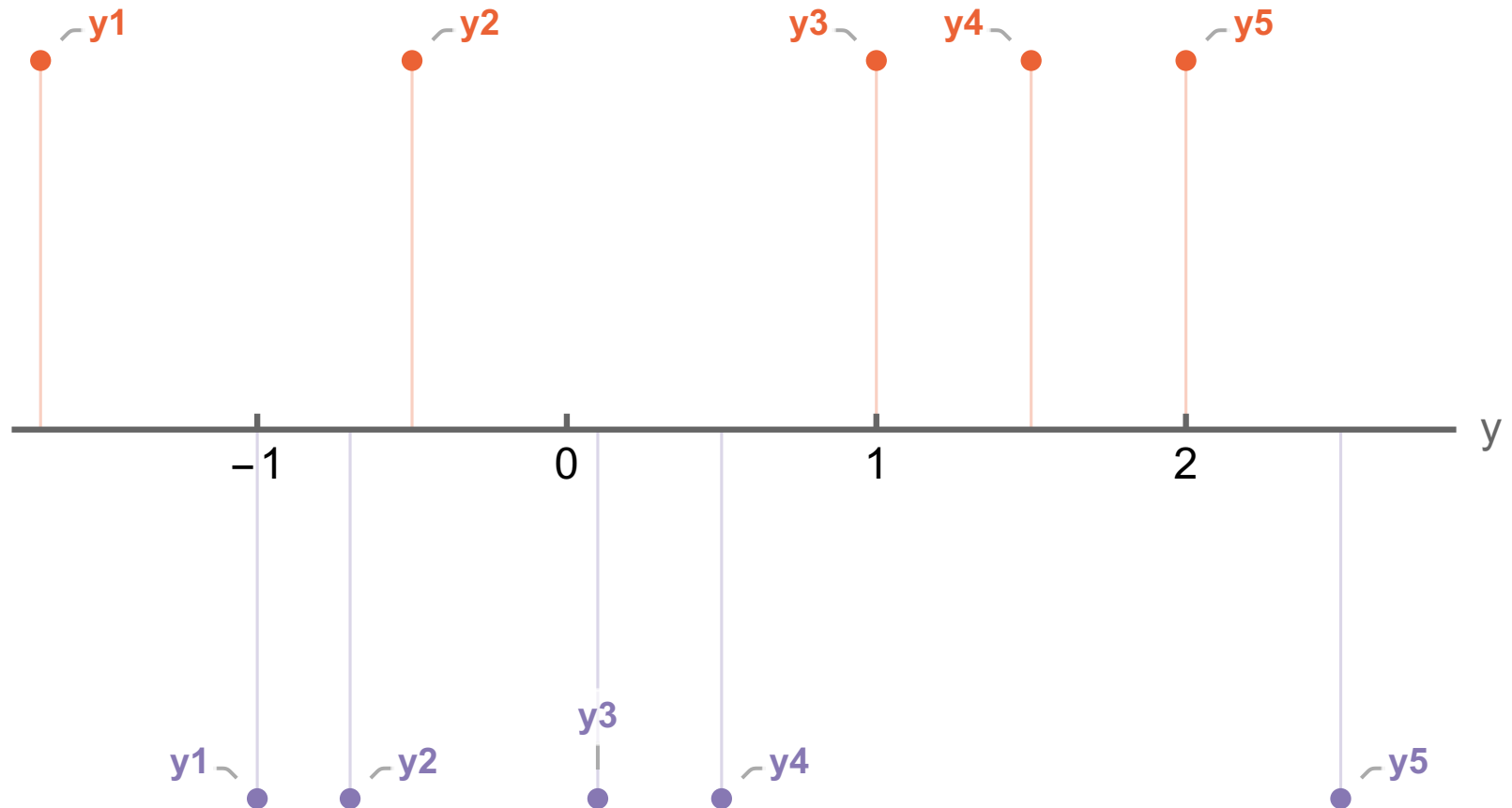
Kinematics

- Consider events with fixed jet multiplicity $N=3+2, 4+2, 5+2$
- Jets in the events must have a $p_T > 20$ GeV to be considered, jets with $p_T < 20$ GeV do not contribute to the jet multiplicity
- The bounding jets (the most forward/backward jets) have $20 < p_T < 30$ GeV and $30 < p_T < 40$ GeV (and the reverse)
- The jets can have rapidity y such that $-4.7 < y < 4.7$
- The rapidity separation of the outermost jets was selected to be $3 < \Delta Y < 4$ and in one case $3.9 < \Delta Y < 4$
- anti- k_T with $R=0.4$ was used as implemented in fastjet
- MSTW2008nnlo PDF (no particular reason, was used in MN studies)

An example with $N=5$ (3+2)

jet ● rapidities of event i

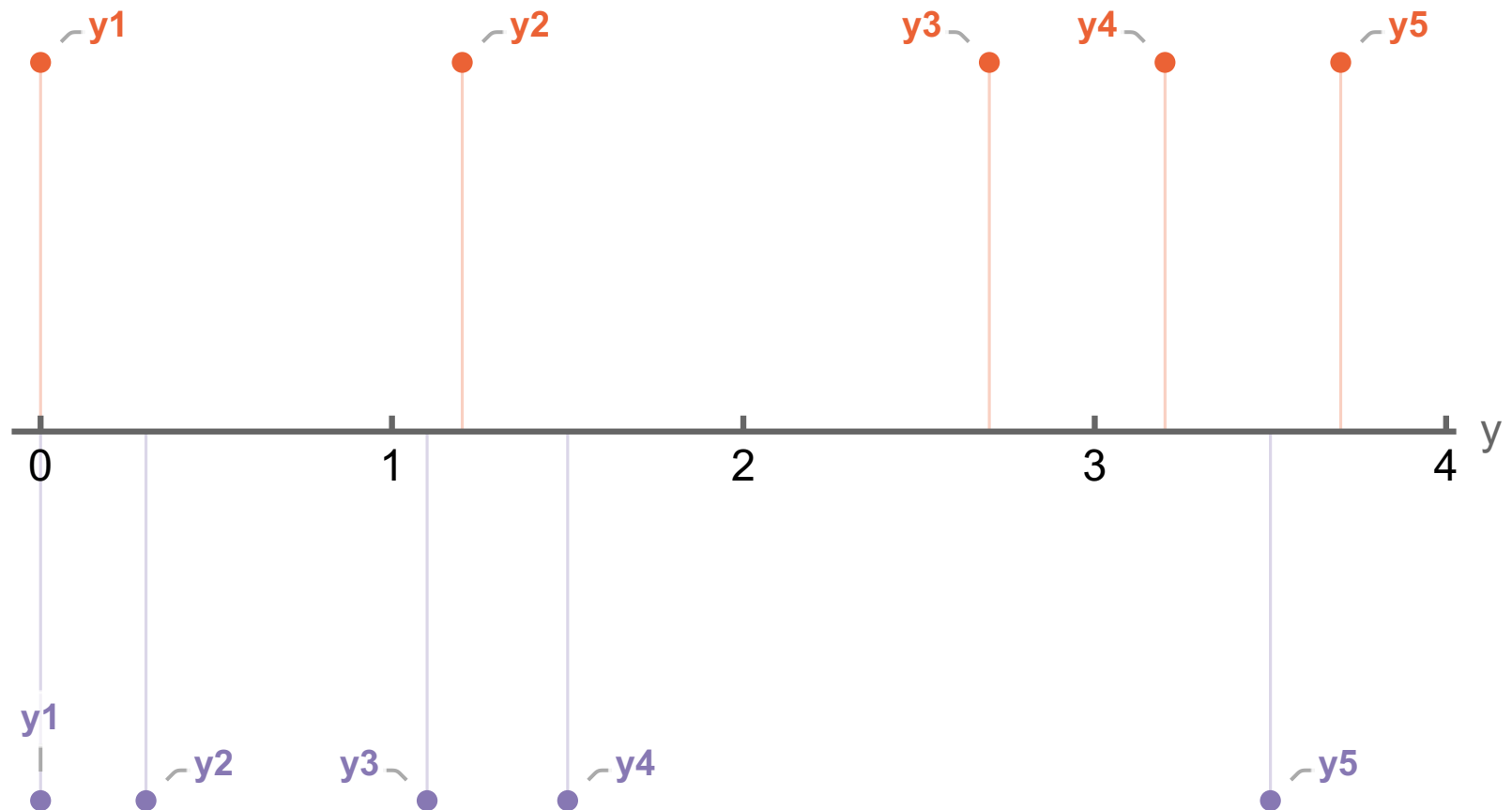
jet ● rapidities of event j



Shift the rapidities such that $y_1=0$

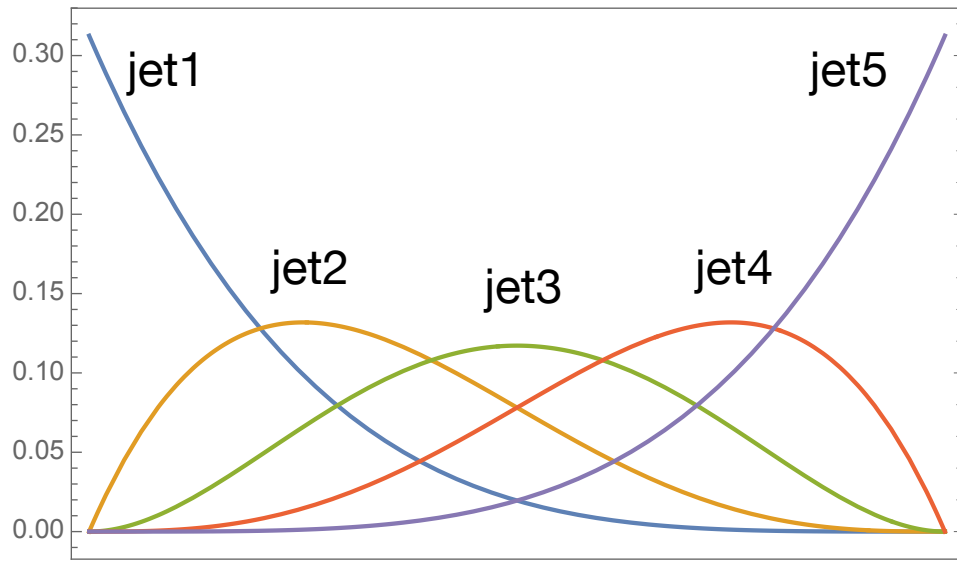
jet ● shifted rapidities of event i

jet ● shifted rapidities of event j

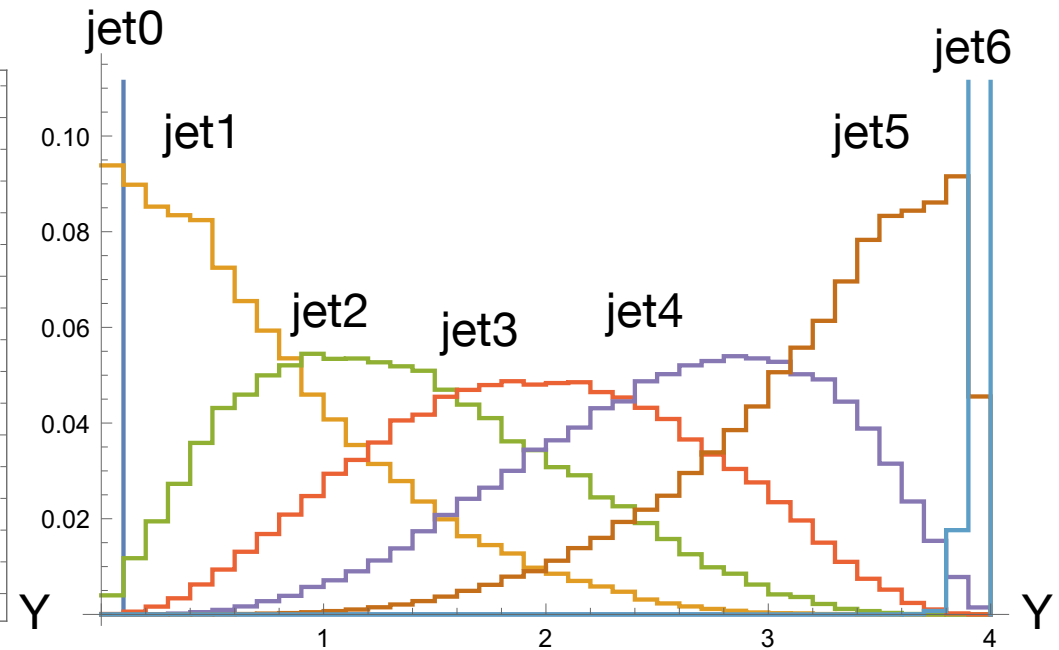


Rapidity distributions for $N=5+2$

$3.9 < \Delta Y < 4$

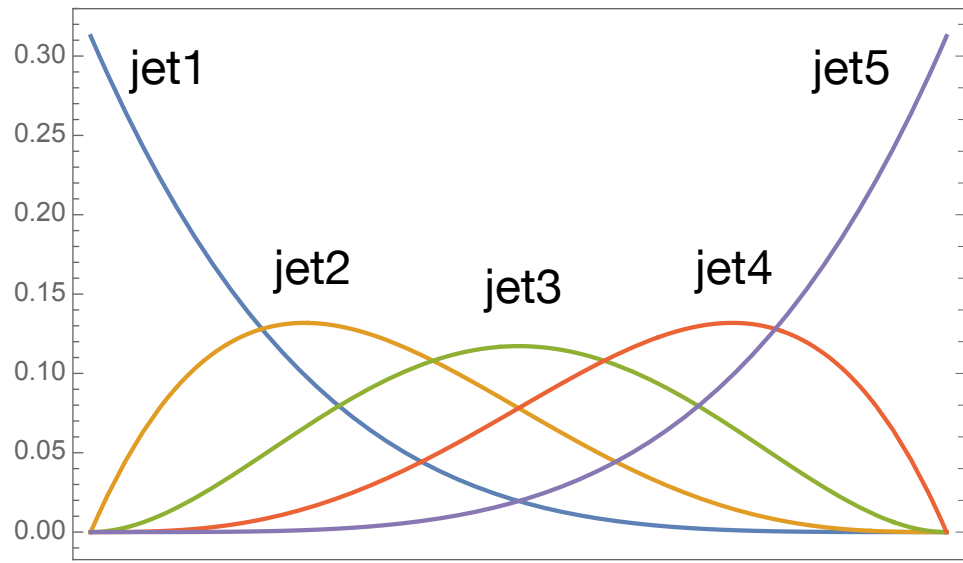


Chew-Pignotti, $N = 5+2$

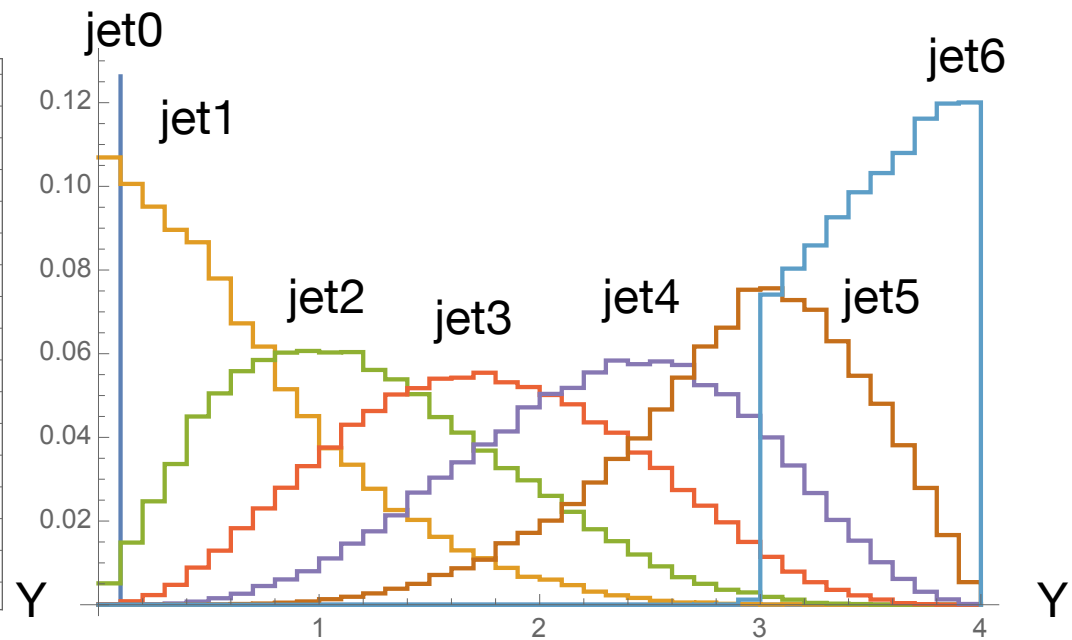


BFKLex, $N = 5+2$

Rapidity distributions for $N=5+2$ $3 < \Delta Y < 4$

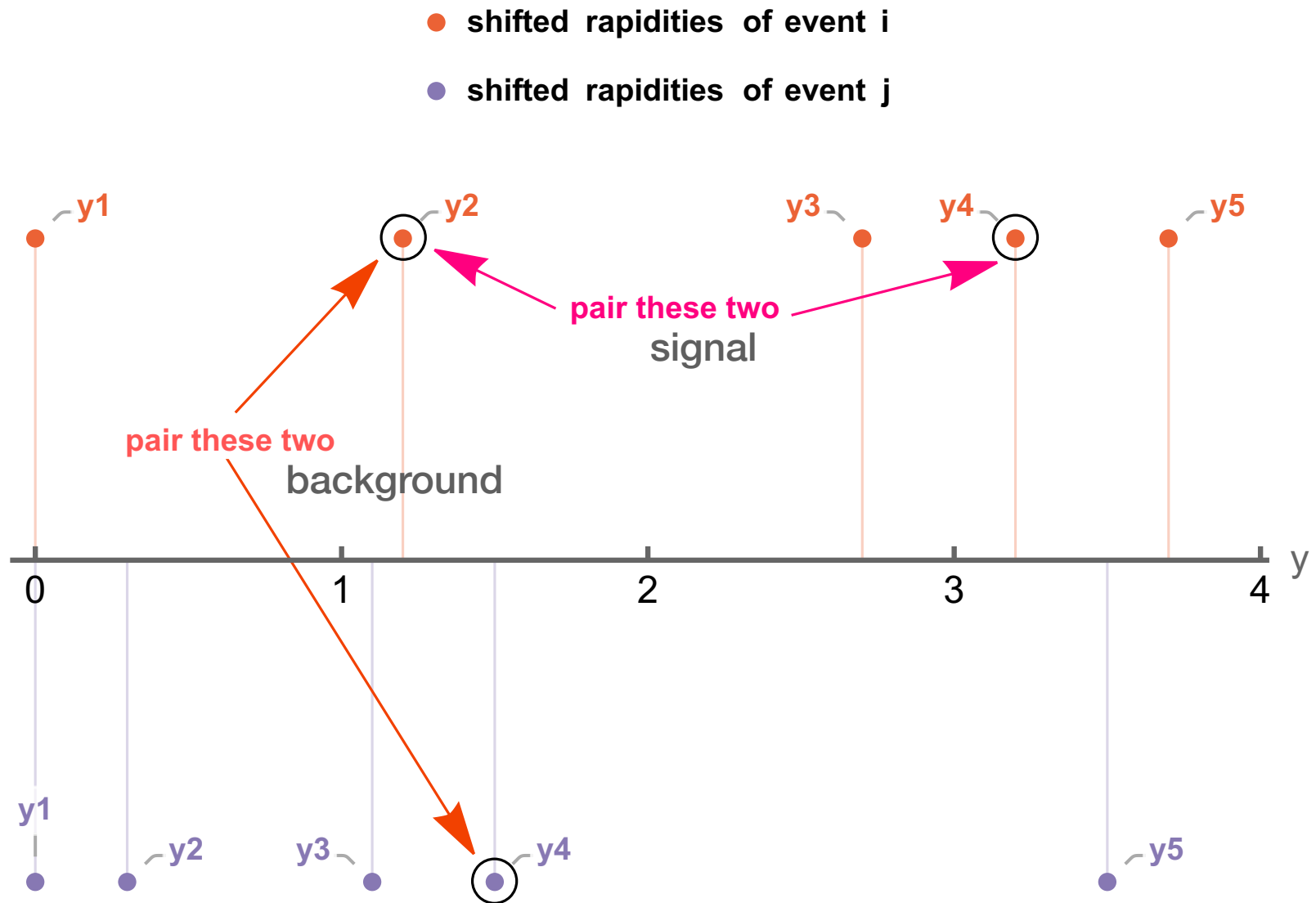


Chew-Pignotti, $N = 5+2$



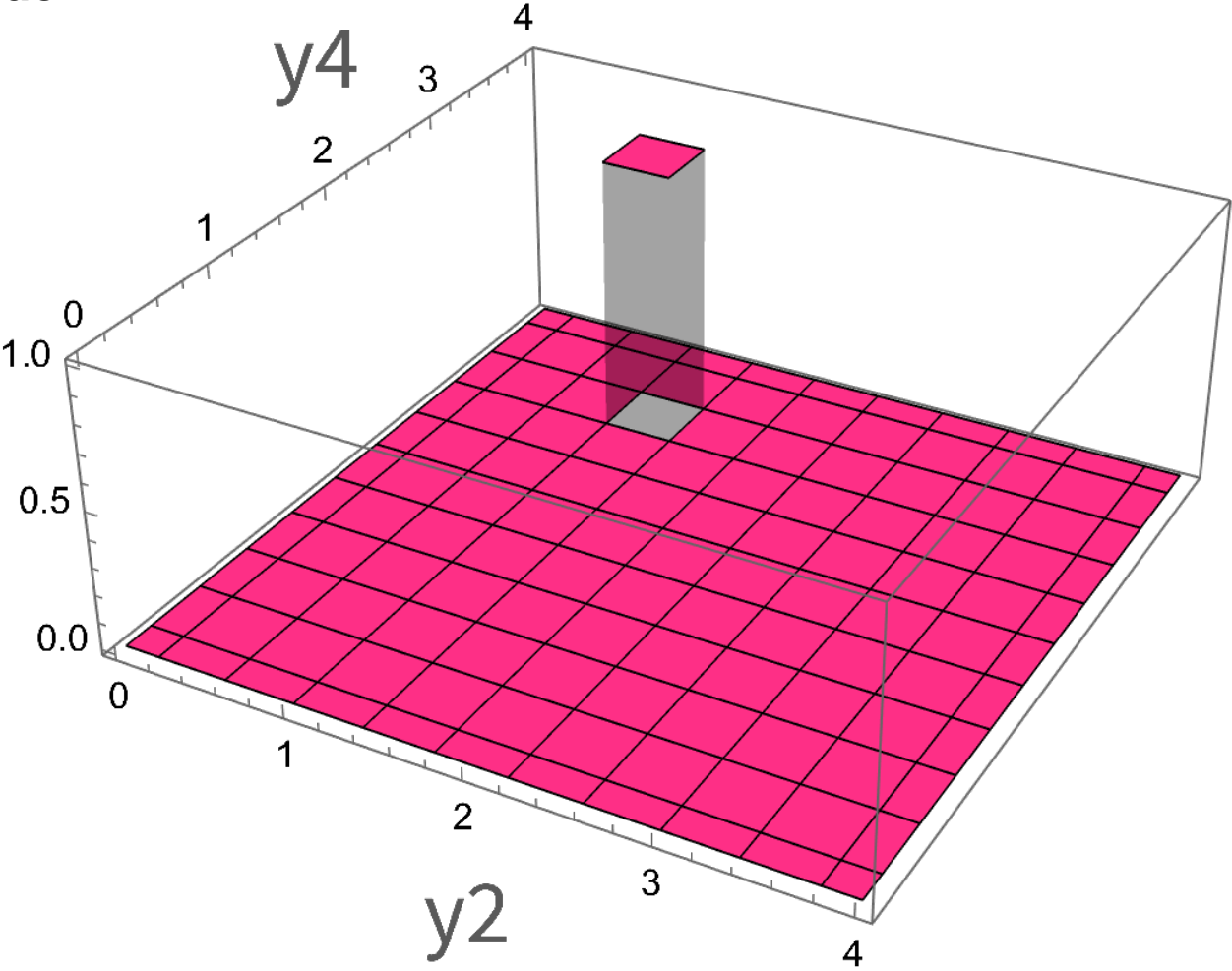
BFKLex, $N = 5+2$

Signal and background distributions



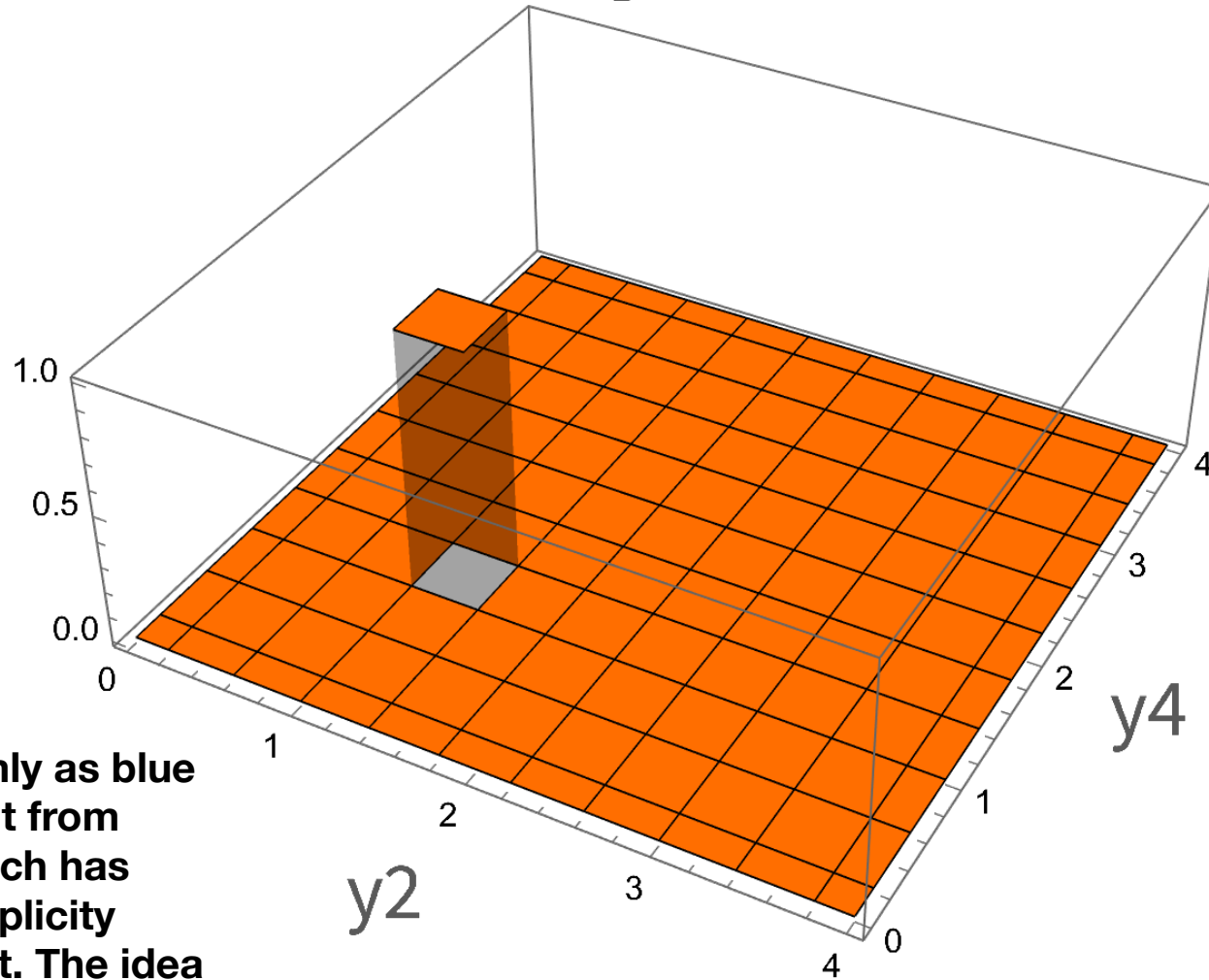
binning the Signal

Here we bin y_2, y_4 from
the orange jets in the
previous slide



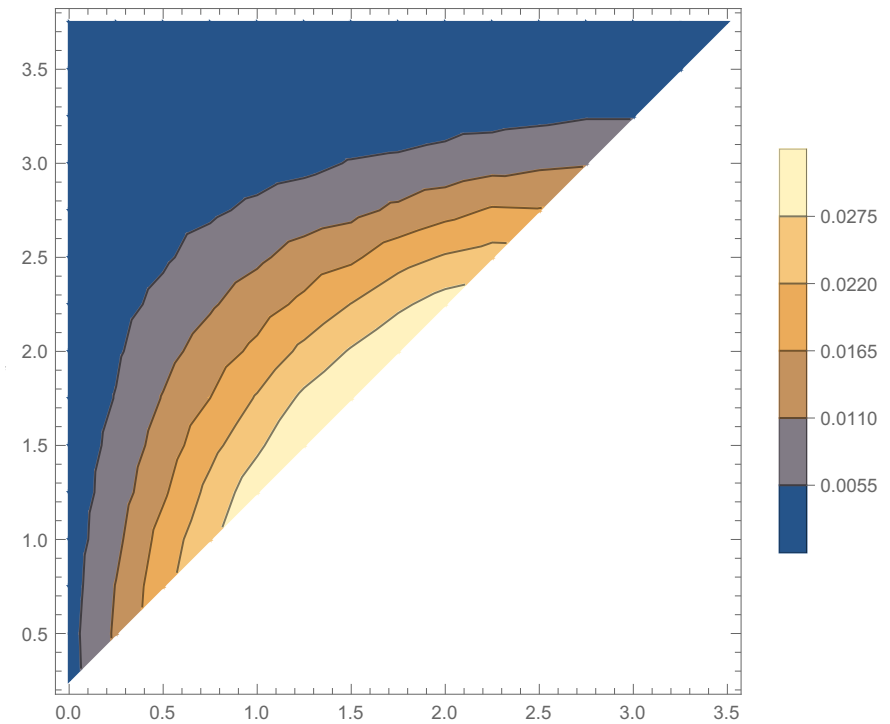
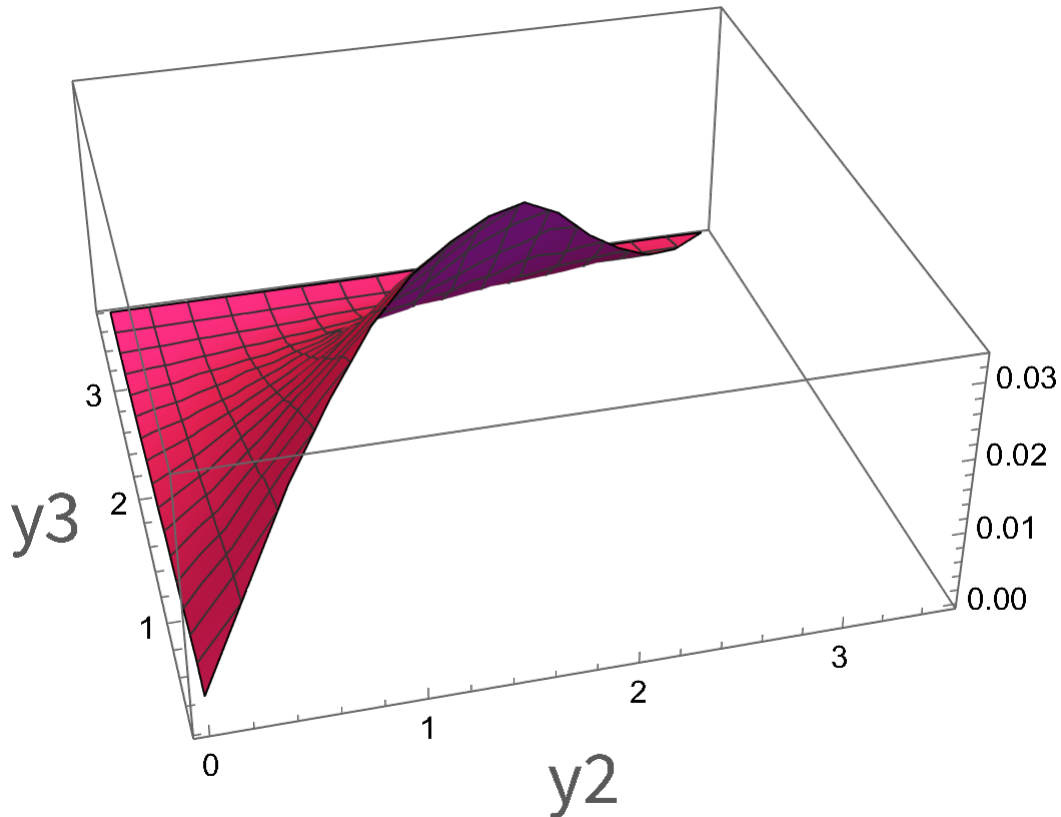
binning the Background

Here we bin y_2 from the orange event and y_4 from the blue event two slides ago.



We choose randomly as blue event any event from the dataset which has the same multiplicity as the orange event. The idea is that y_2 from one event and y_4 from another event should not be correlated.

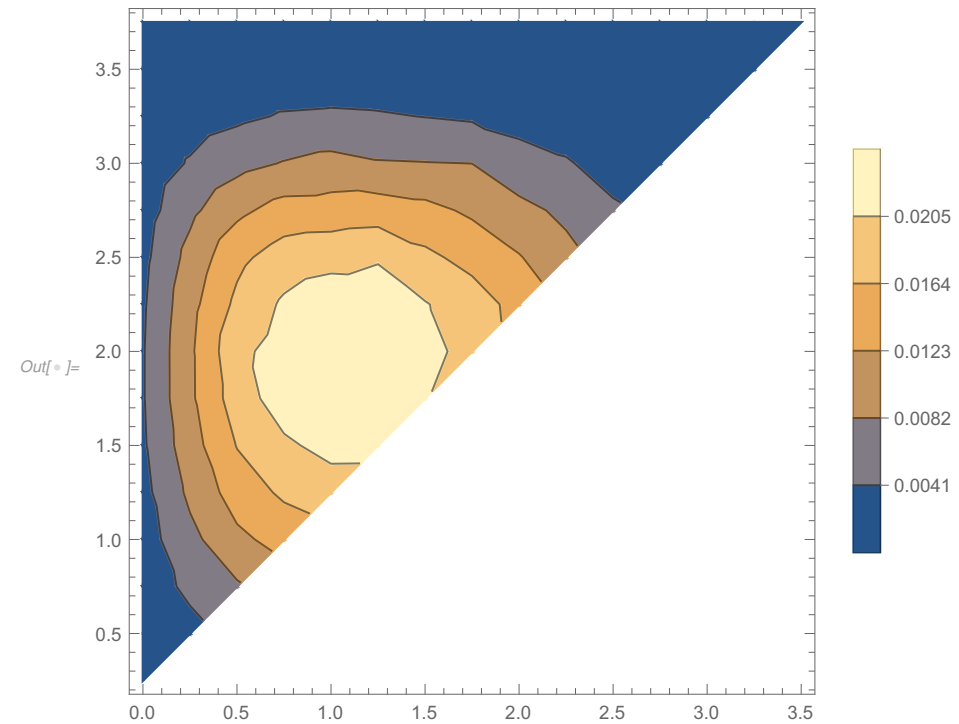
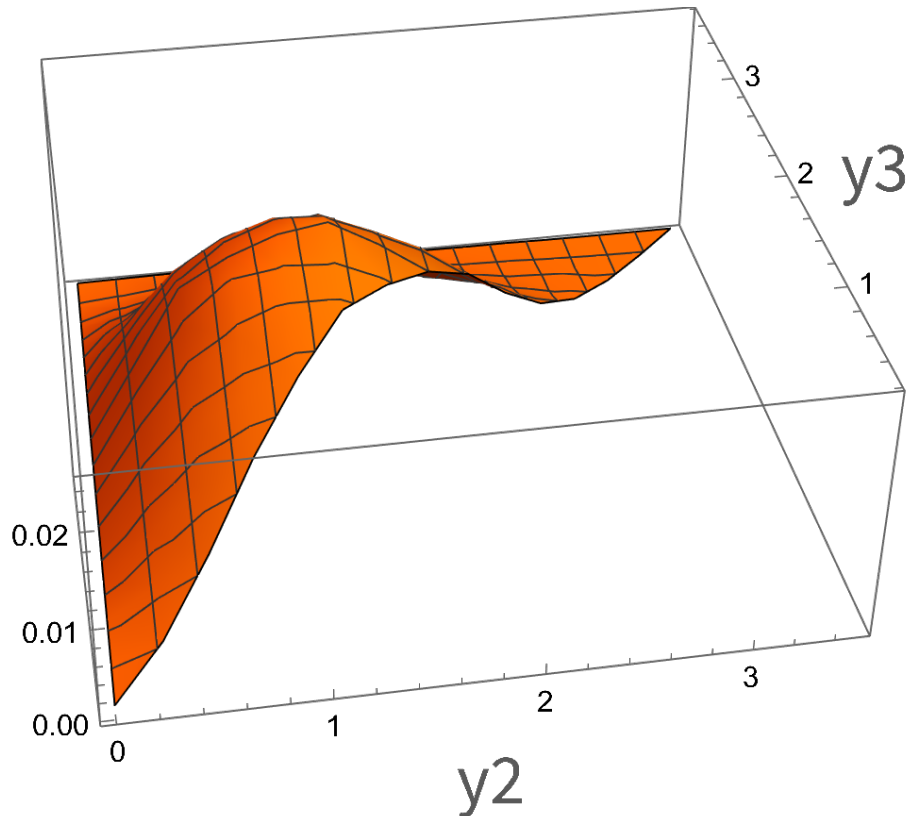
(y_2, y_3) signal distribution, $N = 4+2$



with
BFKLex

(y_2, y_3) background distribution

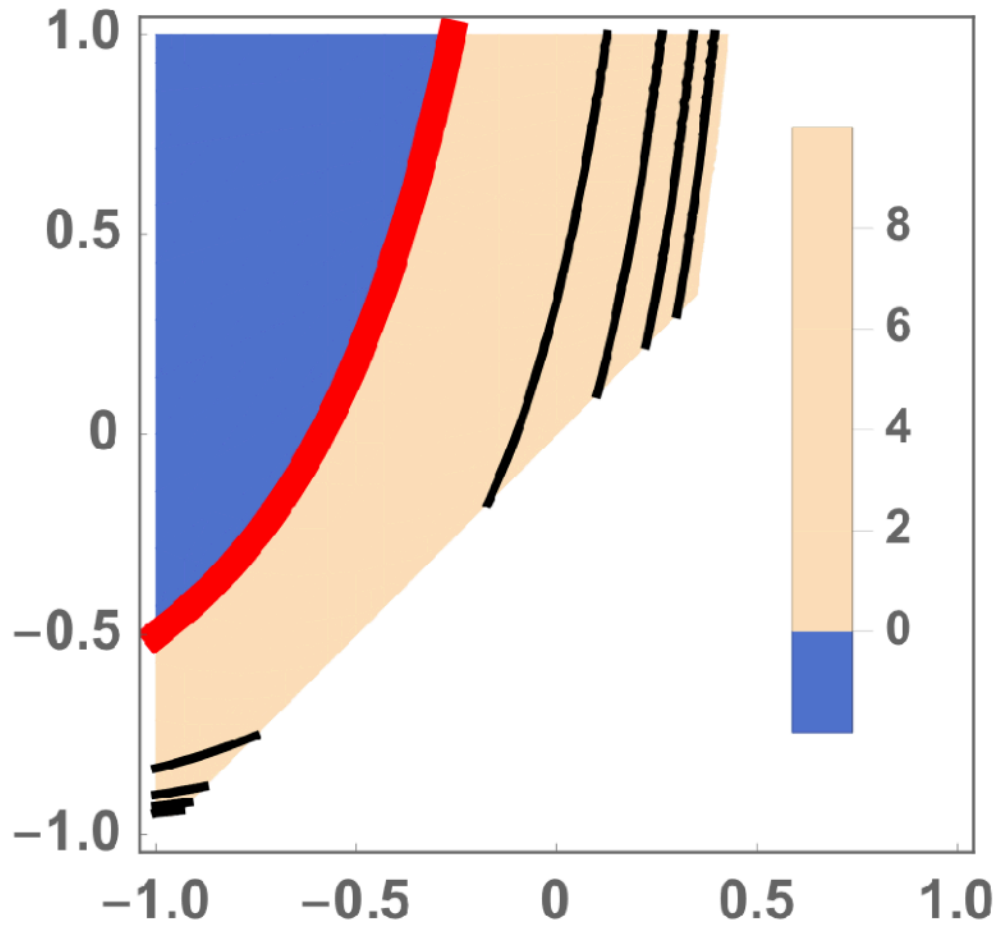
$$N = 4+2$$



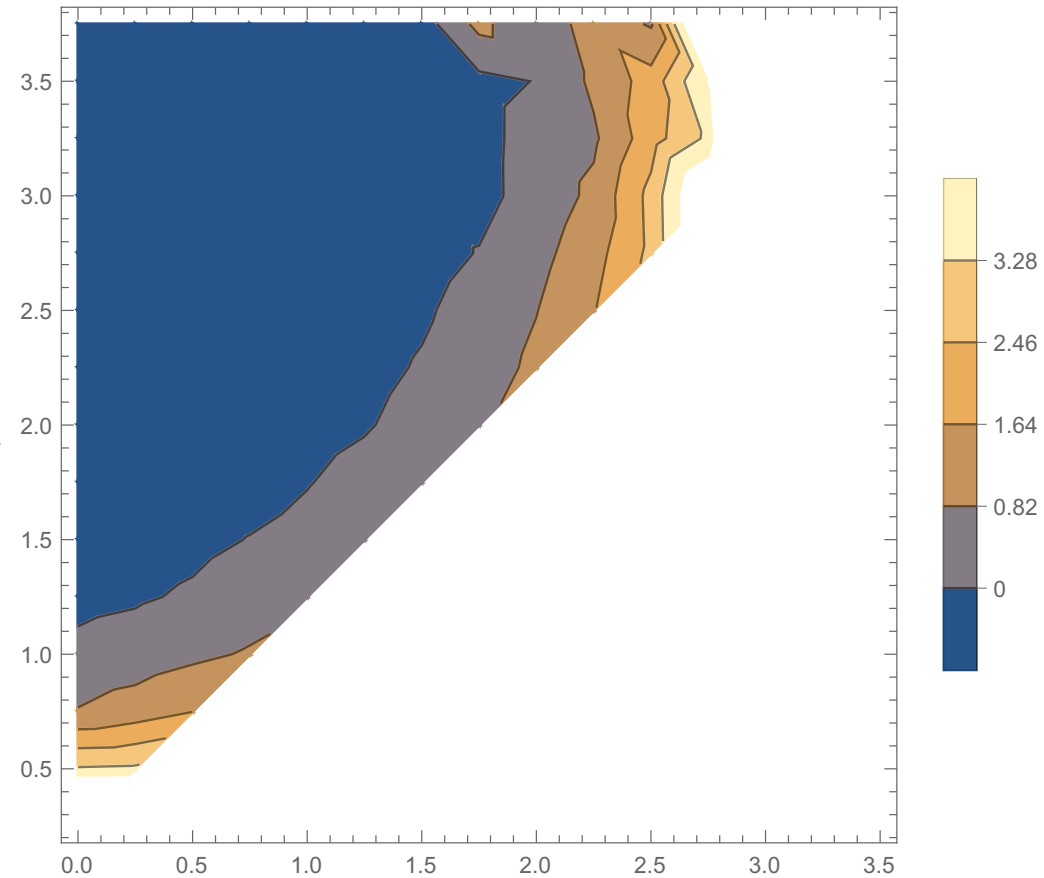
with
BFKLex

Full-run for (y_2, y_3) correlation

$$N = 4+2$$



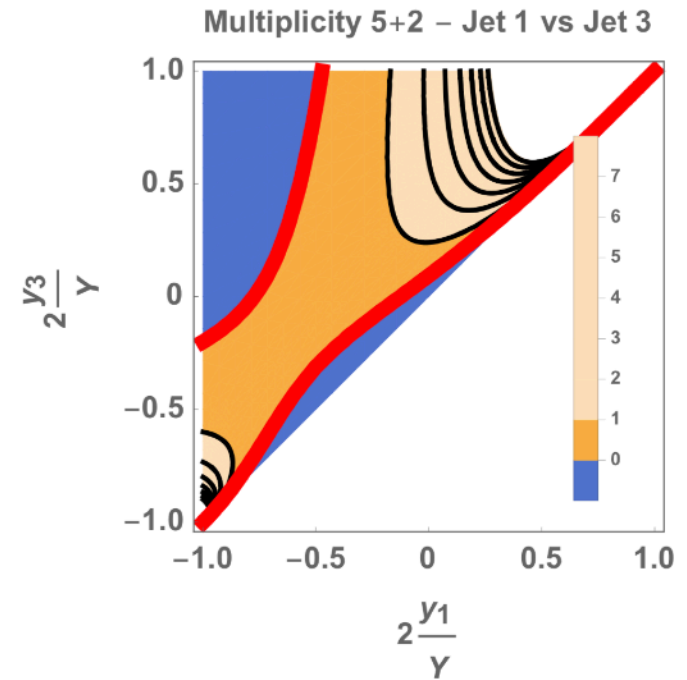
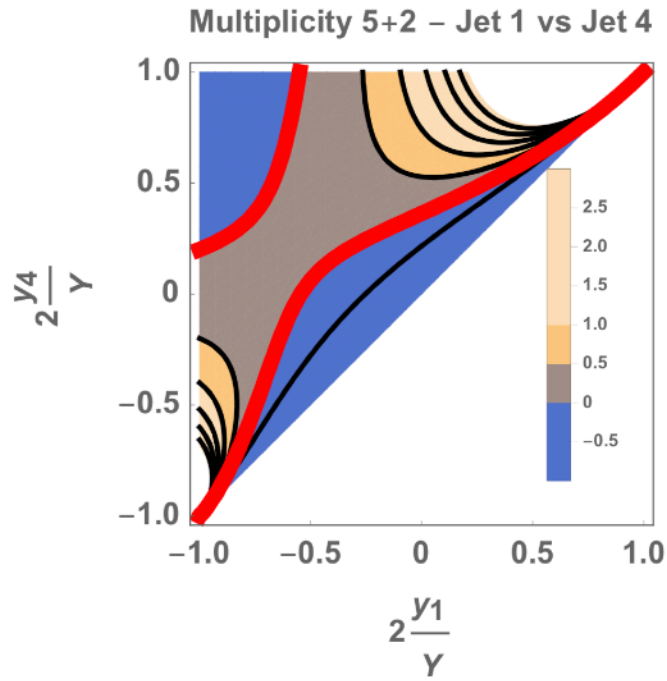
Chew-Pignotti



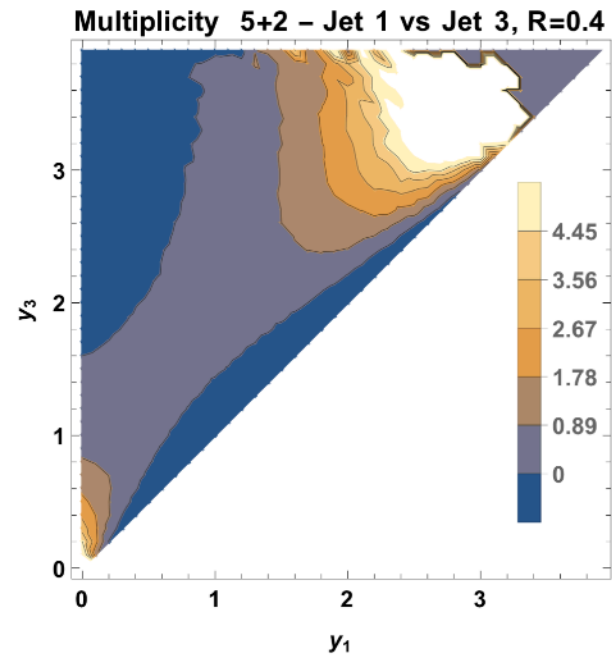
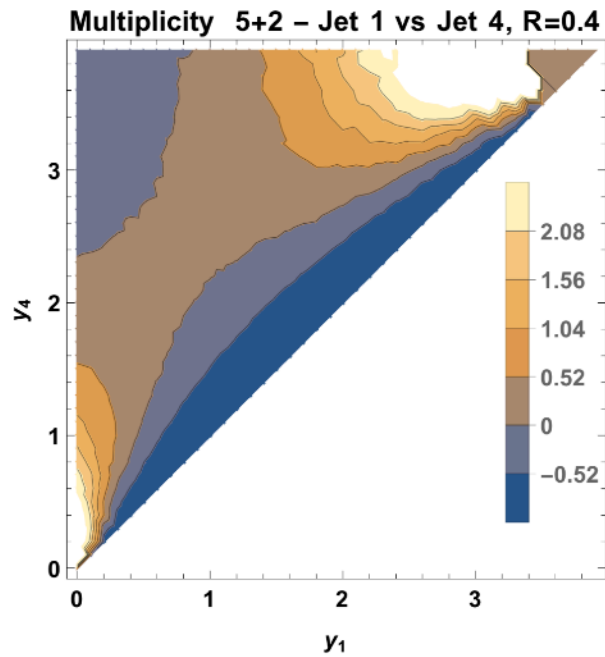
BFKLex

Partonic level run

Chew-Pignotti



BFKLex



Mueller-Navelet jets

New Observables

Compare fixed order+parton shower versus BFKL

- Use a process for which in principle resummation is relevant. Here, **dijet production (Mueller-Navelet jets)**. These are jets widely separated in rapidity with similar p_T where also other jets are allowed at rapidities in between the two bounding jets.
- Use **BFKLex** to calculate the BFKL prediction for a number of exclusive observables.
- Use NLO matrix elements from **POWHEG** with **Pythia** parton shower to calculate the prediction for the same observables.

Kinematics

- Cuts:

$$p_{\perp 0} \in [30; 40] \text{ GeV}$$

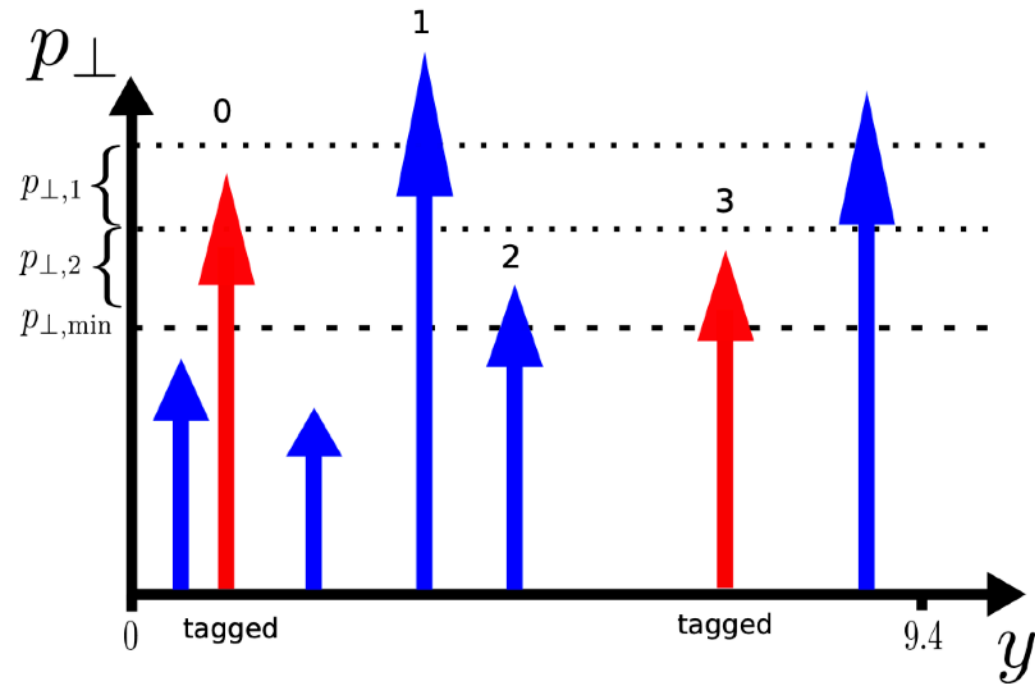
$$p_{\perp n-1} \in [20; 30] \text{ GeV}$$

$$p_{\perp \text{min}} \geq 20 \text{ GeV}$$

$$y \in [-4.7; 4.7]$$

- Maximize $|y_{n-1} - y_0|$ in tagging

Important note: For the comparison, we fix the final jet multiplicity to take the values $N=5, 6, 7$



The high-energy radiation pattern from BFKLex with double-log collinear contributions

- Introduce three quantities related to the jet activity along the ladder. These characterize uniquely the event (but not fully). Consider the following (and variations)

- average p_t

$$\langle p_t \rangle = \frac{1}{N} \sum_{i=1}^N |p_{t_i}|$$

- average azimuthal angle

$$\langle \phi \rangle = \frac{1}{N} \sum_{i=1}^N \phi_i$$

- rapidity ratio between subsequent jets

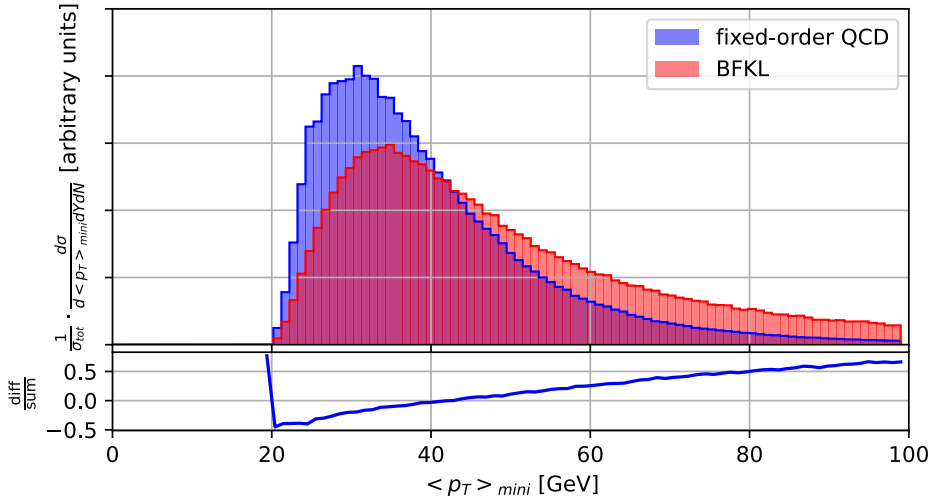
$$\langle \mathcal{R}_y \rangle = \frac{1}{N-1} \sum_{i=1}^{N-1} \frac{y_i}{y_{i+1}}$$

- rapidity ratios weighted with transverse momenta

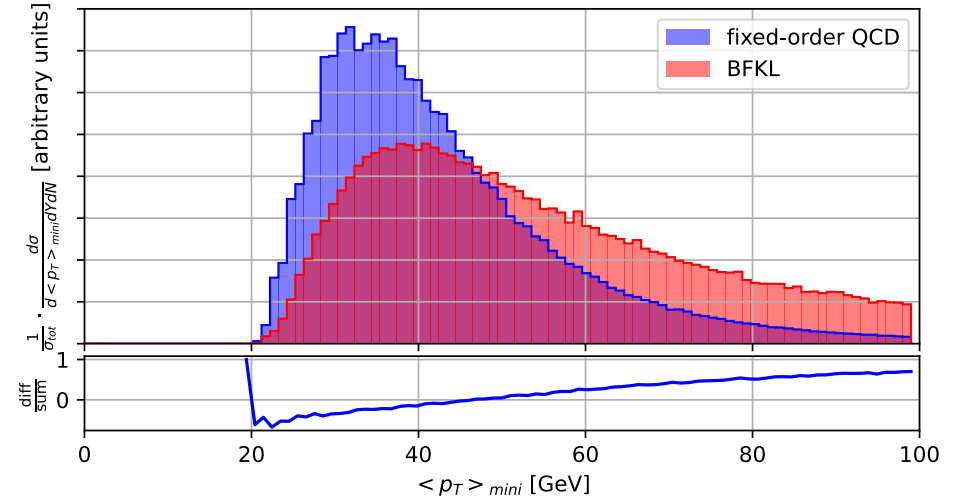
$$\langle \mathcal{R}_{ky} \rangle = \frac{1}{N-1} \sum_{i=1}^{N-1} \frac{p_{t_{i+1}}}{p_{t_i}} e^{y_{i+1}-y_i}$$

Results

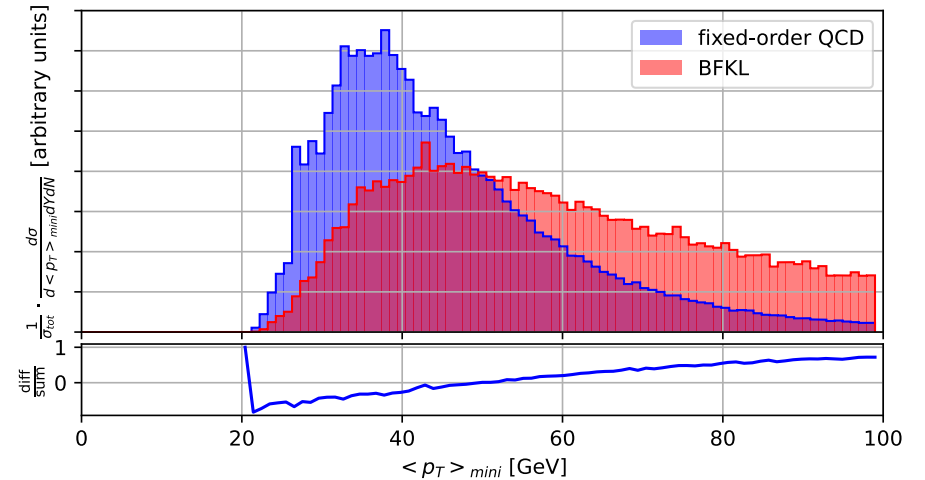
QCD NLO POWHEG + Pythia, $|\eta| \leq 4.7$, $R = 0.5$,
 $p_{T,1} \in [30:40]$ GeV, $p_{T,2} \in [20:30]$ GeV, $p_{T,mini} \geq 20$ GeV
 $Y \in [1;10]$ $N = 5$



QCD NLO POWHEG + Pythia, $|\eta| \leq 4.7$, $R = 0.5$,
 $p_{T,1} \in [30:40]$ GeV, $p_{T,2} \in [20:30]$ GeV, $p_{T,mini} \geq 20$ GeV
 $Y \in [1;10]$ $N = 6$



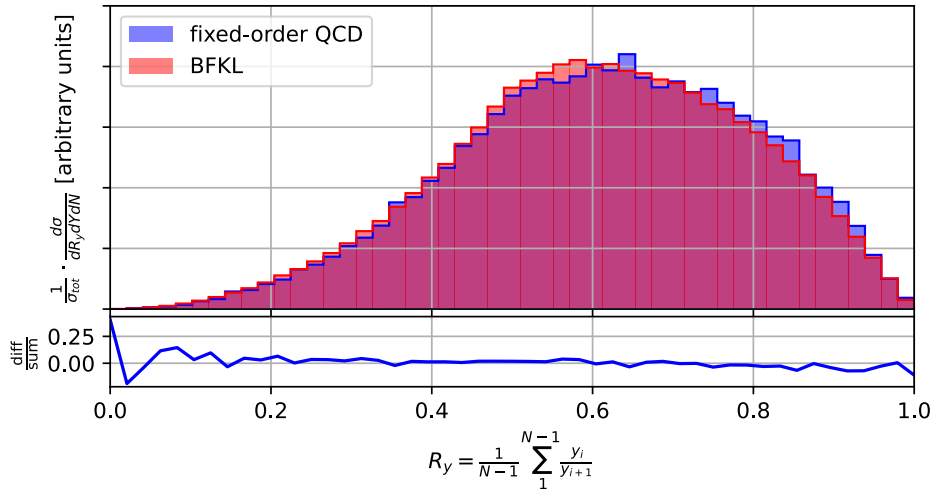
QCD NLO POWHEG + Pythia, $|\eta| \leq 4.7$, $R = 0.5$,
 $p_{T,1} \in [30:40]$ GeV, $p_{T,2} \in [20:30]$ GeV, $p_{T,mini} \geq 20$ GeV
 $Y \in [1;10]$ $N = 7$



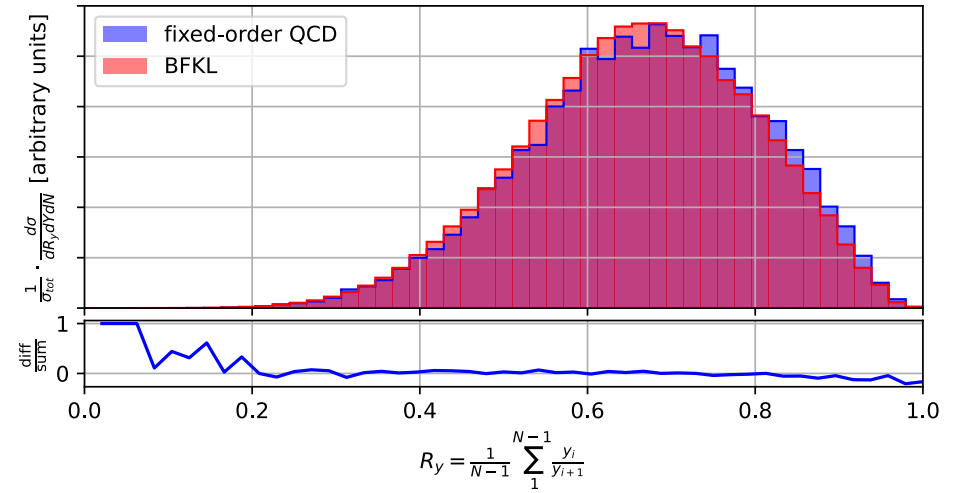
$$\langle p_t \rangle = \frac{1}{N} \sum_{i=1}^N |p_{t_i}|$$

Results

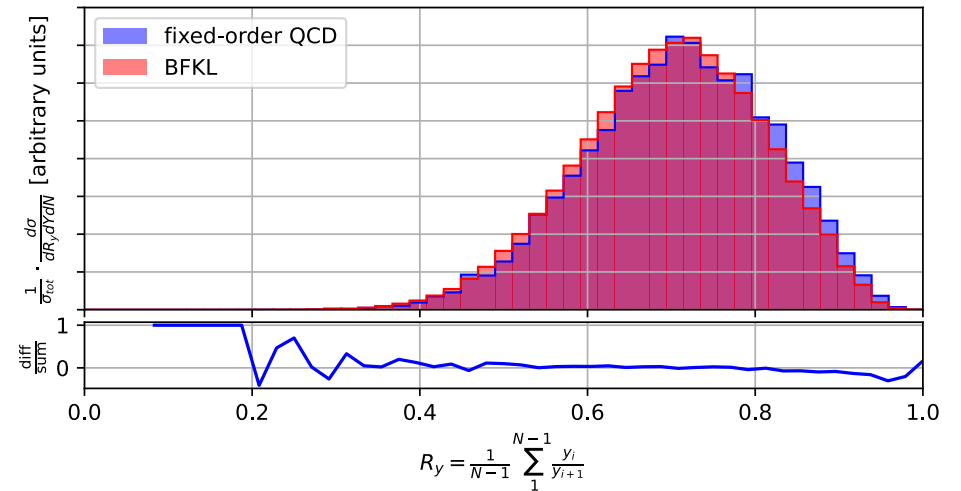
QCD NLO POWHEG + Pythia, $|\eta| \leq 4.7$, $R = 0.5$,
 $p_{T,1} \in [30:40]$ GeV, $p_{T,2} \in [20:30]$ GeV, $p_{T,mini} \geq 20$ GeV
 $Y \in [1;10]$ $N = 5$



QCD NLO POWHEG + Pythia, $|\eta| \leq 4.7$, $R = 0.5$,
 $p_{T,1} \in [30:40]$ GeV, $p_{T,2} \in [20:30]$ GeV, $p_{T,mini} \geq 20$ GeV
 $Y \in [1;10]$ $N = 6$



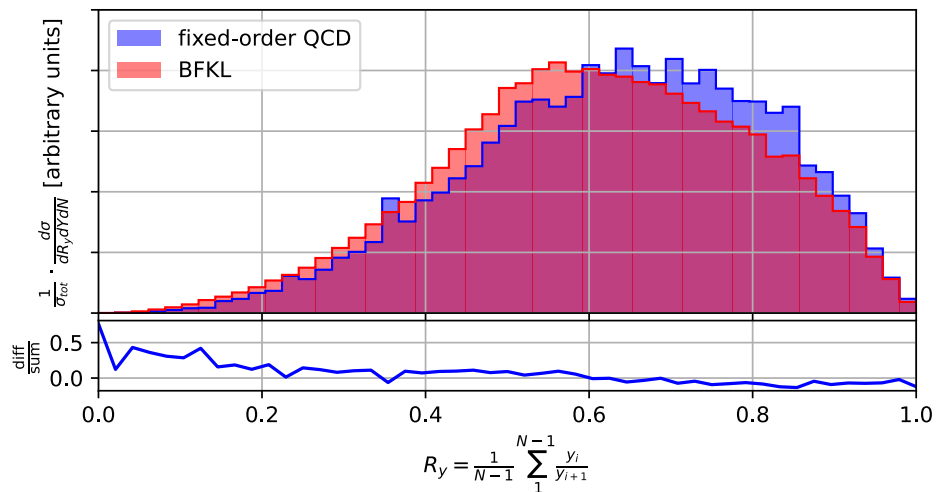
QCD NLO POWHEG + Pythia, $|\eta| \leq 4.7$, $R = 0.5$,
 $p_{T,1} \in [30:40]$ GeV, $p_{T,2} \in [20:30]$ GeV, $p_{T,mini} \geq 20$ GeV
 $Y \in [1;10]$ $N = 7$



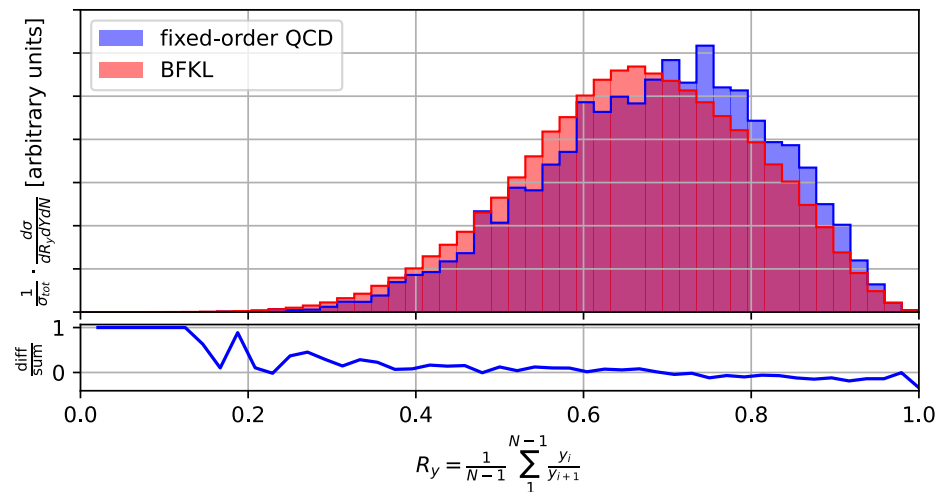
$$\langle R_y \rangle = \frac{1}{N-1} \sum_{i=1}^{N-1} \frac{y_i}{y_{i+1}}$$

Results

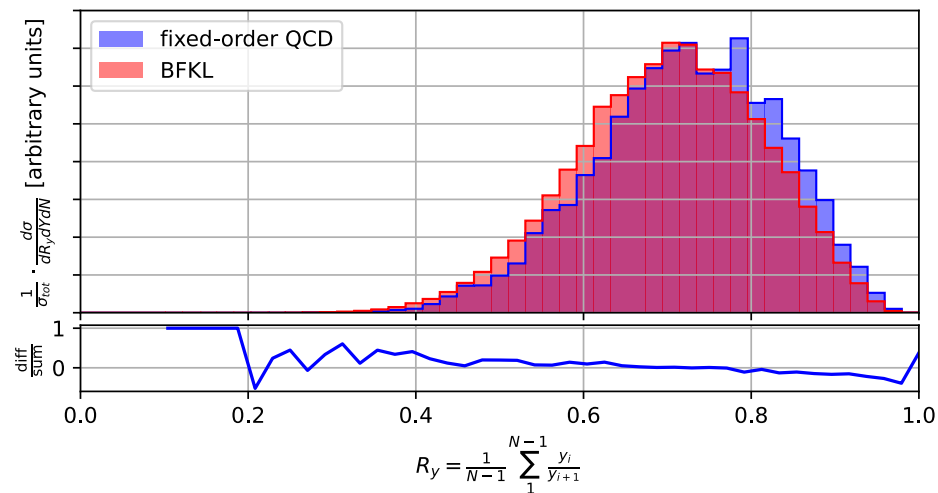
QCD NLO POWHEG + Pythia, $|\eta| \leq 4.7$, $R = 0.5$,
 $p_{T,1} \in [30:40]$ GeV, $p_{T,2} \in [20:30]$ GeV, $p_{T,mini} \geq 20$ GeV
 $Y \in [5;10]$ $N = 5$



QCD NLO POWHEG + Pythia, $|\eta| \leq 4.7$, $R = 0.5$,
 $p_{T,1} \in [30:40]$ GeV, $p_{T,2} \in [20:30]$ GeV, $p_{T,mini} \geq 20$ GeV
 $Y \in [5;10]$ $N = 6$



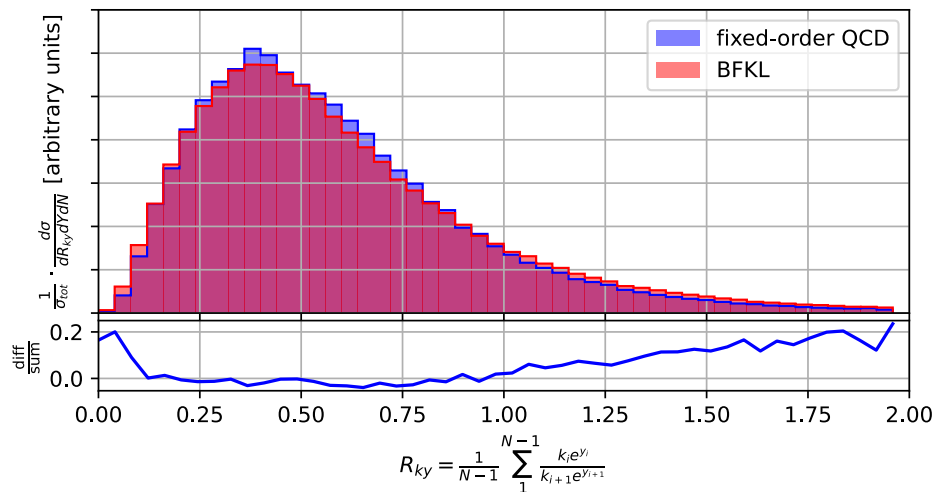
QCD NLO POWHEG + Pythia, $|\eta| \leq 4.7$, $R = 0.5$,
 $p_{T,1} \in [30:40]$ GeV, $p_{T,2} \in [20:30]$ GeV, $p_{T,mini} \geq 20$ GeV
 $Y \in [5;10]$ $N = 7$



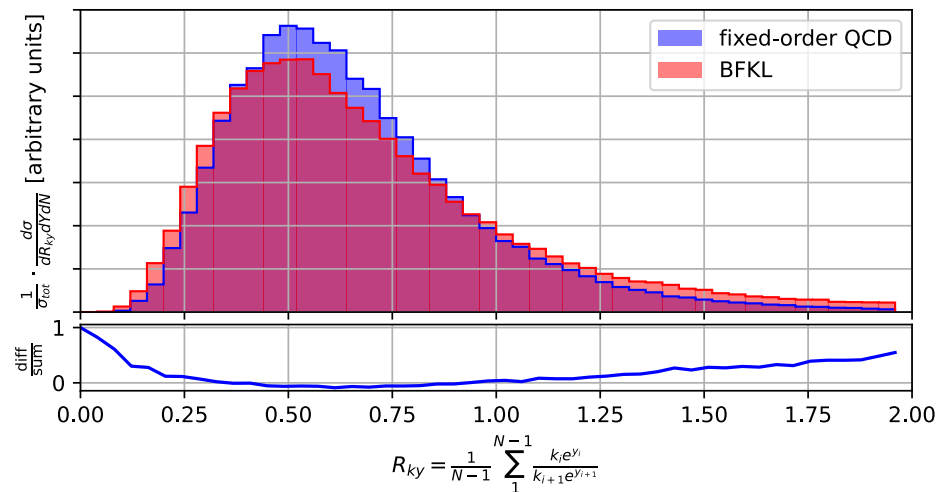
$$\langle R_y \rangle = \frac{1}{N-1} \sum_{i=1}^{N-1} \frac{y_i}{y_{i+1}}$$

Results

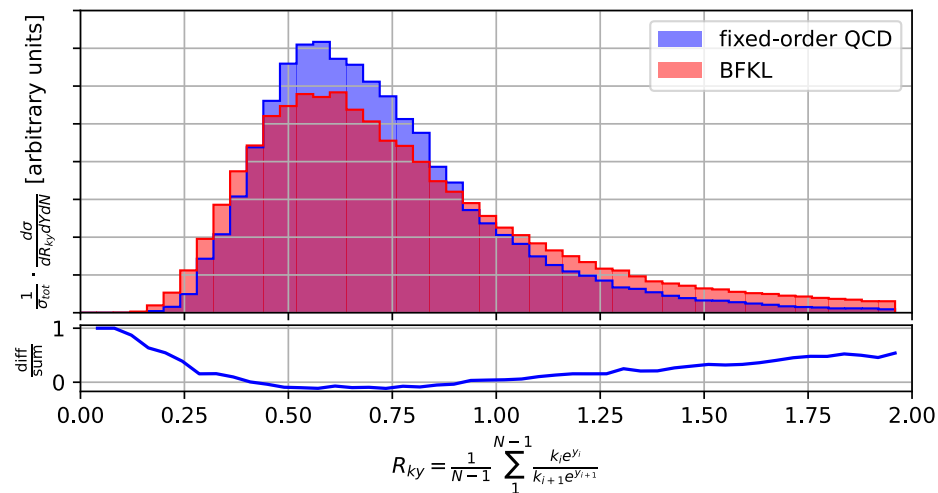
QCD NLO POWHEG + Pythia, $|\eta| \leq 4.7$, $R = 0.5$,
 $p_{T,1} \in [30:40]$ GeV, $p_{T,2} \in [20:30]$ GeV, $p_{T,mini} \geq 20$ GeV
 $Y \in [1;10]$ $N = 5$



QCD NLO POWHEG + Pythia, $|\eta| \leq 4.7$, $R = 0.5$,
 $p_{T,1} \in [30:40]$ GeV, $p_{T,2} \in [20:30]$ GeV, $p_{T,mini} \geq 20$ GeV
 $Y \in [1;10]$ $N = 6$



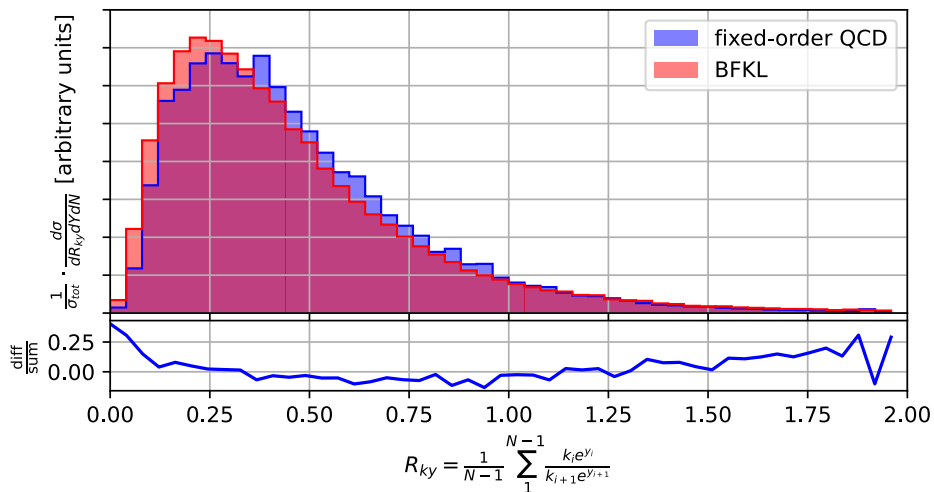
QCD NLO POWHEG + Pythia, $|\eta| \leq 4.7$, $R = 0.5$,
 $p_{T,1} \in [30:40]$ GeV, $p_{T,2} \in [20:30]$ GeV, $p_{T,mini} \geq 20$ GeV
 $Y \in [1;10]$ $N = 7$



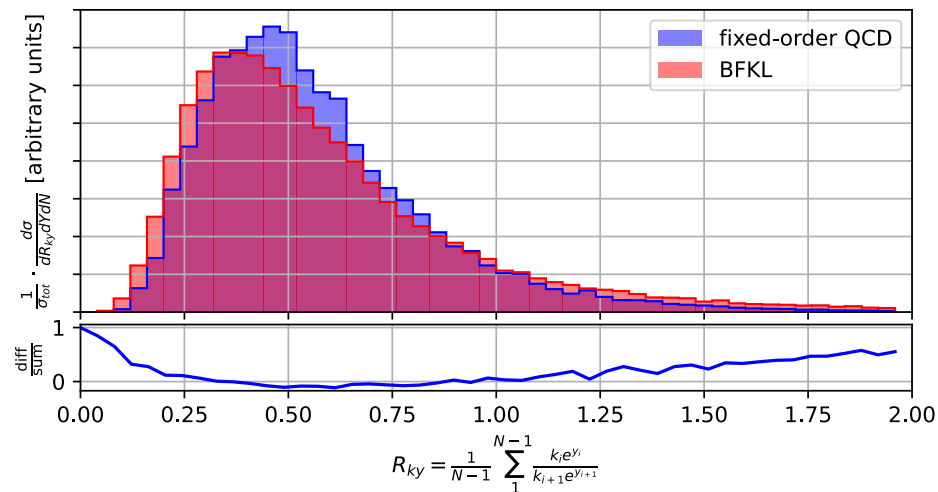
$$\langle \mathcal{R}_{ky} \rangle = \frac{1}{N-1} \sum_{i=1}^{N-1} \frac{p_{t_i}}{p_{t_{i+1}}} e^{y_i - y_{i+1}}$$

Results

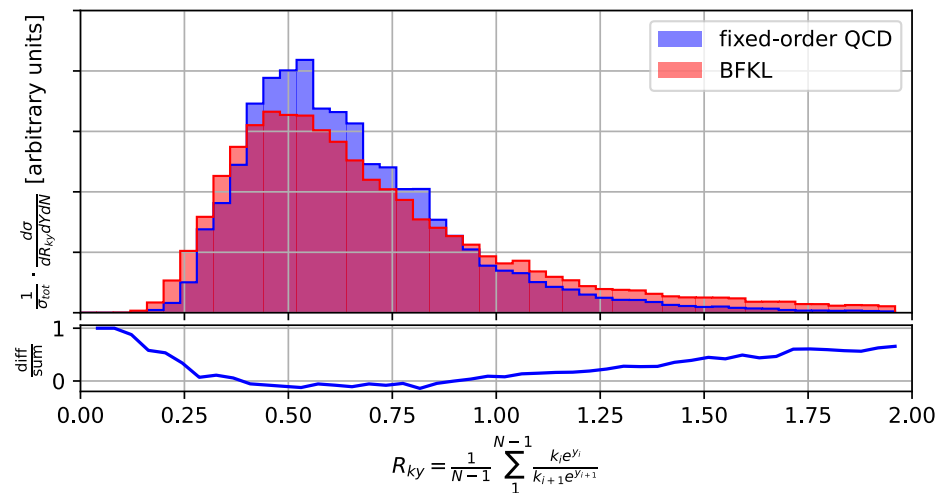
QCD NLO POWHEG + Pythia, $|\eta| \leq 4.7$, $R = 0.5$,
 $p_{T,1} \in [30:40]$ GeV, $p_{T,2} \in [20:30]$ GeV, $p_{T,mini} \geq 20$ GeV
 $Y \in [5;10]$ $N = 5$



QCD NLO POWHEG + Pythia, $|\eta| \leq 4.7$, $R = 0.5$,
 $p_{T,1} \in [30:40]$ GeV, $p_{T,2} \in [20:30]$ GeV, $p_{T,mini} \geq 20$ GeV
 $Y \in [5;10]$ $N = 6$



QCD NLO POWHEG + Pythia, $|\eta| \leq 4.7$, $R = 0.5$,
 $p_{T,1} \in [30:40]$ GeV, $p_{T,2} \in [20:30]$ GeV, $p_{T,mini} \geq 20$ GeV
 $Y \in [5;10]$ $N = 7$



$$\langle \mathcal{R}_{ky} \rangle = \frac{1}{N-1} \sum_{i=1}^{N-1} \frac{p_{t_i}}{p_{t_{i+1}}} e^{y_i - y_{i+1}}$$